Tampere University

NGUYEN, THI QUYNH NGA

IN VITRO ANTI-GLIOBLASTOMA ACTIVITY OF NOVEL QUINIC ACID DERIVATIVES

Master of Science Thesis
Faculty of Engineering and Natural Sciences
Examiner: Adjunct Professor. Meenakshisundaram Kandhavelu
Examiner: Assistant Professor. Ville Santala
April 2020

ABSTRACT

NGUYEN, THI QUYNH NGA: *In vitro* anti-glioblastoma activity of novel quinic acid derivatives.
Master of Science Thesis
Tampere University
Bioengineering
April 2020

Glioblastoma multiforme, the common malignant tumor with a worst prognosis, is considered as the most challenging in brain tumor treatment. Variety of therapies are currently used for glioblastoma treatment including the combination of surgery with radiotherapy and chemotherapy. Chemotherapy is effective treatment for patients, however risky due to serious side effects is observed. In specific, temozolomide (TMZ), the most prevalent effective anti-glioblastoma agent in chemotherapy, is currently utilized during or after radiation therapy, unveils drawbacks such as the development of TMZ resistance and bone marrow suppression. As a consequence, this treatment results in reduction in mortality rate. It is expected that the appearance of novel chemotherapeutic agents, newly synthesized anticancerous compound, could be both effective and safe to address these obstacles. As such, quinic acid and their derivatives recently has grasped the notable attention in treatment of cancers by a broad-spectrum of preeminent properties such as antioxidation, anti-inflammation, anticancer, which were demonstrated by afore studies. In addition, nicotinamide, which is converted from quinic acid is proven to induce apoptosis via inhibition of Nuclear Factor- Kappa B, indicates the efficacy of quinic acid in cancer treatment. Therefore, the quinic acid derivatives with the modifications to enhance their function towards glioblastoma treatment, were chemically synthesized and examined as potential chemotherapeutic agents. In this study, the total of sixteen novel quinic acid derivatives were screened for preliminary cytotoxicity, in which AK-4 was defined as the top lead compound with cell growth inhibition of 90.12 ± 5.10 % utilizing cytotoxic assay. Further studies were conducted in an attempt to evaluate the anticancer properties of AK-4 towards proliferation, migration, and reactive oxygen species (ROS) generation of two glioblastoma cell lines LN229 and SNB19 as well as influence on the growth of non-cancerous cells, MEF. AK-4 showed the low inhibitory potency (IC_{50}), which were determined as 10.66 ± 4.71 μM and 28.22 ± 9.87 μM in LN229 and SNB19, respectively. In term of time-dependent effect, there was a slight rise in inhibitory ability of AK-4 against glioblastoma cells growth; nevertheless, it is observed that AK-4 was less cytotoxic with respect to sodium orthovanadate, positive control, over 72 h drug exposure. Additionally, at high concentration of 100 μM, AK-4 still be considered to be less harmful to non-cancerous cells, MEF with IC_{50} of 54.35 ± 10.18 % cell growth inhibition, which was significantly lower than the IC_{50} of two glioblastoma cell lines. Moreover, scratch assay revealed that AK-4 exhibited comparable inhibitory effect on migration of the cells, in both cell lines with respect to sodium orthovanadate over 8 hours. The evaluation of ROS level observed in both cell lines suggests the association of AK-4 with induction of cancer cell death. The findings in this study provided preliminary evidence suggesting that AK-4, a quinic acid derivative, could be promising chemotherapeutic agents, especially in glioblastoma treatment. This study also has laid the groundwork for further investigations aimed at developing more effective anticancer drugs.

Key words: glioblastoma multiforme, anticancer, quinic acid, apoptosis, cytotoxicity.

PREFACE

Above all, I wish to express my sincere gratitude to my supervisor Adjunct Professor. Meenakshisundaram Kandhavelu, who allowed me to work on this thesis topic. I have been blessed because I have learnt a lot of knowledge in research field as well as received training with ambition and patience from him. In truth, I could not achieve this thesis successfully without his guidance.

I also would like to extend my deep appreciation to my second supervisor Assistant Professor. Ville Santala for his permission to carry out this thesis as well as valuable responses to my work.

I am extremely grateful to Hien Le, Phuong Doan for their kind guidance throughout research project and also to Tien Nguyen and Kenna Brown for being great coworkers. Especially, Hien Le has always been helping and supporting me during laboratory time. In addition, I really appreciate Kenna Brown, who got involved in several experiments in this thesis and made nights at laboratory more fun.

All my love and thanks to my family in Hoi An, Vietnam and my beloved friends for their encouragement and faith.

Finally, this thesis is accomplished amid novel coronavirus pandemic worldwide and it is unforgettable to me. Wish everyone around the world all the best and coronavirus may end soon. Stay healthy and happy!

Tampere, 29th April 2020

Nguyen Thi Quynh Nga

CONTENTS

LIST OF TABLES

LIST OF FIGURES

LIST OF SYMBOLS AND ABBREVIATIONS

ANOVA	Analysis of variance
Ca^{2+}	Calcium ions
CAD	Caspase-activated DNAse
DCF	2′,7′-dichlorofluorescein
FBS	Fetal Bovine Serum
H_2DCF	2',7'-dichlorodihydrofluorescein
H_2DCFDA	2',7'-dichlorodihydrofluorescein diacetate
IC_{50}	Half maximal inhibition concentration
CDF	Cumulative Distribution Function
DMEM	Dulbecco's Modified Eagle Medium
DMSO	Dimethyl sulfoxide
FBS	Fetal Bovine Serum
IAP	Inhibitors of apoptosis protein
PBS	Phosphate Buffered Saline
PCD	Programmed cell death
TMZ	Temozolomide

1. INTRODUCTION

Cancer, caused by gene mutation, is the second-leading reason of mortality globally. In relation to the origin of brain tumors, they are classified generally into primary tumors, and metastatic brain tumors. Glioma is a primary brain tumors and categorized into three major subtypes consisting of astrocytoma (including glioblastoma multiforme), ependymoma and oligodendroglioma in according to specific type of cells [1]. In specific, astrocytomas graded from II to IV class, originate in astrocytes, glia cells having shape of star. Likewise, ependymomas arise from ependymal cells and oligodendrogliomas originate in oligodendrocytes [2].

Glioblastoma multiforme, also called glioblastoma, is the most prevalent malignant brain tumor and classified as grade IV as specified by 2016 CNS WHO classification [3]. With regards to glioblastoma treatments, there are mainly four options including aggressive surgery, radiation therapy, chemotherapy; and tumor treating fields; notwithstanding, combination of therapies is considered as hallmark of cancer treatment as well as glioblastoma treatment. In spite of advances in treatment, GBM patients possess a poor prognosis and the drawback of current treatments is reduction of mortality rate. Uncontrollable growth as well as migration of glioblastoma cells resulting in the recurrence of tumor and the diffusion of tumor cells, are considered as two among crucial reasons causing treatment failures [4]. Specifically, Temozolomide (TMZ) in chemotherapy, recognized as the most effective agent for glioblastoma treatment and utilized during or after radiation therapy, reveals downsides; for example, the development of TMZ resistance and bone marrow suppression [5,6]. Whereby, the identification and development of novel chemotherapeutic agents, which are effective and safe to address these obstacles, will pave a promising path to glioblastoma treatment.

Quinic acid is a biochemical intermediate in the shikimate biosynthetic pathway providing precursors for aromatic amino acids [7]. This biosynthetic pathway is found only in plants and microorganisms, therefore, mammals including human are not able to synthesize quinic acid, only supplement it via diet and nutritionally elevate the production of major ingredients including tryptophan and nicotinamide, which in turn results in induction of DNA repair and inhibition of Nuclear Factor- Kappa B (NF-κB) [8–12]. In recognition of

NF-κB as transcription factors in key biological processes, inhibition of NF-κB can suppress proliferation of cancer cells and induce apoptosis [13]. In addition, the quinic acid and their derivatives, especially phenolic acid derivatives, have shown broad-spectrum antitumor, antioxidant, anti-inflammation, neuroprotection and hepatoprotection on treatment for cancers including oral, prostate cancers and inflammatory as well as central nervous system-related diseases [14,15]. For instance, (-)-4-O-(4-O-β-D-glucopyranosylcaffeoyl)quinic acid is demonstrated to display anticancer capability against human colon cancer [16]. 5-*O*-caffeoyl-quinic acid is another example which has shown antitumor activity against various type of cancer as liver and lung cancers [17]. Thereby, quinic acid derivatives could be novel potential chemotherapeutic agents against glioblastoma treatment and are recently synthesized as well as assessed their efficacy widely.

Novel anti-tumor agents are identified and designed for targeted therapy or by computational screening methods [18]. The clinical assessment will unveil which novel anticancer agent possesses therapeutic values. Nonetheless, the stumbling-blocks of clinical assessment in relation to ethical, economic, and medical restriction as well as limited number of patients for trial promote successful development of experimental assessment (*in vitro*), in which the therapeutic value of anticancer agent is primarily examined, mainly by cell-based models. The potential agents are in turn tested *in vivo*. In this thesis, quinic acid derivatives were studied *in vitro* to assess their anti-glioblastoma activity. The sixteen quinic acid derivatives was first tested against glioblastoma multiforme cell line LN229. The further examinations were performed to ascertain the corresponding characteristics in two glioblastoma multiforme cell lines including LN229 and SNB19 in aspects of cell proliferation, migration, reactive oxygen species (ROS) generation under treatment with the top leading derivative. Additionally, mouse embryonic fibroblast (noncancerous brain cells) and patient-derived primary glioblastoma multiforme (GBM) cells were also utilized to evaluate the cytotoxicity of this compound.

2. THEORETICAL BACKGROUND

The development of anticancer agents plays a crucial role in cancer therapeutics, especially in chemotherapy, in which anticancer agents are utilized to destroy cancer cells by hindering them from growing and dividing. It is obvious that the identification, development as well as assessment of novel chemotherapeutic agents require understanding the cell cycle as well as cell death programs. Therefore, the goal of this chapter is to show an overview of quinic acid and its derivatives as promising anticancer agents in term of biological activity and synthesis. Moreover, the cell death mechanisms are also delineated to show the working mechanism of anticancer agents towards cancer cells.

2.1 Quinic acid and its derivatives

Quinic acid and its derivatives are compounds containing a quinic acid moiety, which is composed of a cyclohexane ring bearing a carboxylic acid at position 1 and four hydroxyl groups at positions 1,3, 4, and 5 as illustrated in Figure 1A. Quinic acid is a natural compound which can be found widely in plant species as *cinchona* bark, *eucalyptus globulus* bark, *nettle* leaves. Other quinic acid derivatives are also present in plants as chlorogenic acid (Figure 1B) found in coffee bean as well as leaves of *etlingera elatior*, and hydroxycinnamoylquinic acid found in *arnica* flowers [19–21]

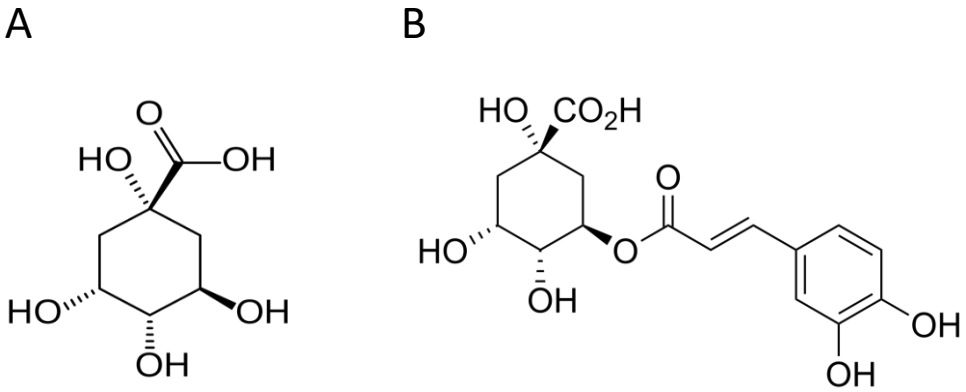

Figure 1. *Chemical structure of quinic acid (A)* [22] *and chlorogenic acid (B)* [23]

In nature, quinic acid could be synthesized from dehydroquinate and shikimate using quinate dehydrogenase and quinate hydrolyase, respectively. Quinic acid is also known

as predecessor for chlorogenate in higher plants (Figure 2). Chlorogenate, partly protecting plant health against the microbial attack and probably becoming promising carbon sources for microbes if this impediment is broken.

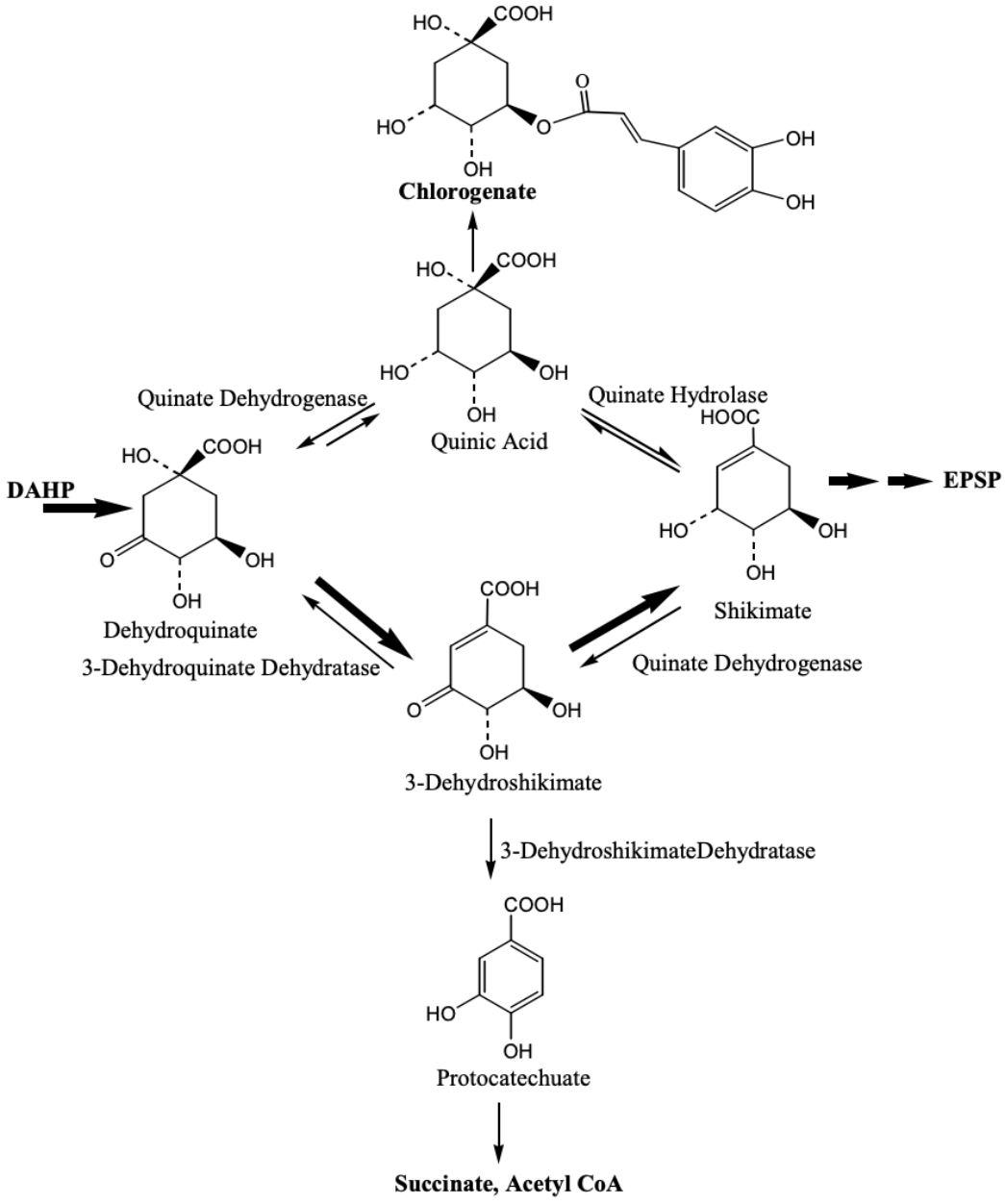

Figure 2. *Biotransformation of quinic acid and shikimate pathway* [24]

Quinic acid is a biochemical intermediate in the shikimate biosynthetic pathway, found only in plants and microorganisms, which provides precursors for aromatic amino acids. In Figure 2, the reactions in shikimate pathway, represented by bold arrows, are catalyzed mainly by 3-deoxy-D-arabino-heptulosonate 7-phosphate synthase (DAHP) and 5-

enolpyruvylshikimate 3-phosphate synthase (EPSP) for synthesis of chorismate ultimately. Chorismate serves as substrate in anabolic sequences to synthesize the aromatic compounds as tyrosine, and tryptophan. Quinic acid is readily degraded into either protocatechuate by fungi and bacterial and then succinate and acetyl-COA or shikimate before entering into shikimate pathway and ultimately synthesizing aromatic compounds.

Recent studies have shown biological activities associated with quinic acid and its derivatives including antitumor, antioxidation, anti-inflammation, neuroprotection, hepatoprotection [24–27]. As an example, the chlorogenic acid, bioconstituent of ethanol extract of *B. vulgaris* fruit was demonstrated to suppress the growth of breast cancer cell line MCF-7. Especially, this compound is also involved in the NF-κB inhibition, being responsible for cancer cell proliferation inhibition and apoptosis induction without affecting the amount of phosphorylated IκB-α, a NF-κB inhibitor. It is also claimed that the development of chlorogenic acid and its related derivatives would be highly competitive because proteasome inhibitors as bortezomib are only approved agents so far for NF-κB inhibition (Figure 3). Meanwhile, quinic acid from flowers of *Moringa oleifera Lam* was reported to hinder the growth of prostate cancer rather than curcumin, a standard therapeutic agent. Methyl 5-caffeoylquinic acid, a predominant constituent from *Saussurea triangulata*, showed neuroprotective effect for neurodegeneration treatment in another study. The quinic acid derivatives with hepatoprotective activity in methanolic extract of compositae were proved as potent agents against the growth of hepatitis B virus. As reported in another study, extracts of *Uncaria tomentosa* containing quinic acid esters have been found to have anti-inflammatory.

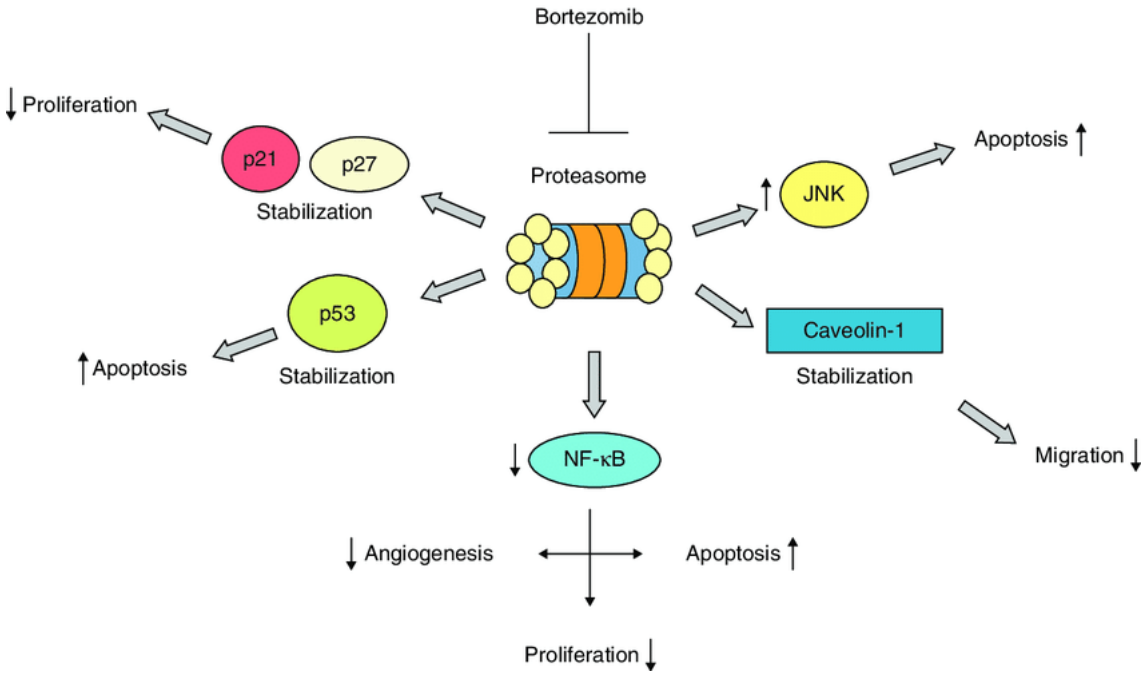

Figure 3. *Inhibition of NF-κB signal pathway by proteasome* [28]

Despite the fact that quinic acid and its derivatives have shown potential effects, the bioavailability of them in animal were low according to several scientists. Specifically, it is found out that chlorogenic acid (CGA) poorly absorbed through alimentary tract in human. In rat, CGA was difficult to absorb through small intestine and was then hydrolyzed in cecum by microflora (Figure 4). Regrading to quinic acid in all species, gut flora played a crucial in conversion of quinic acid to benzoic acid as depicted Figure 4 [24]. Thereby, development of stable quinic acid derivatives retaining biological activities would be also a criterion in discovery and development of alternative anticancer agents.

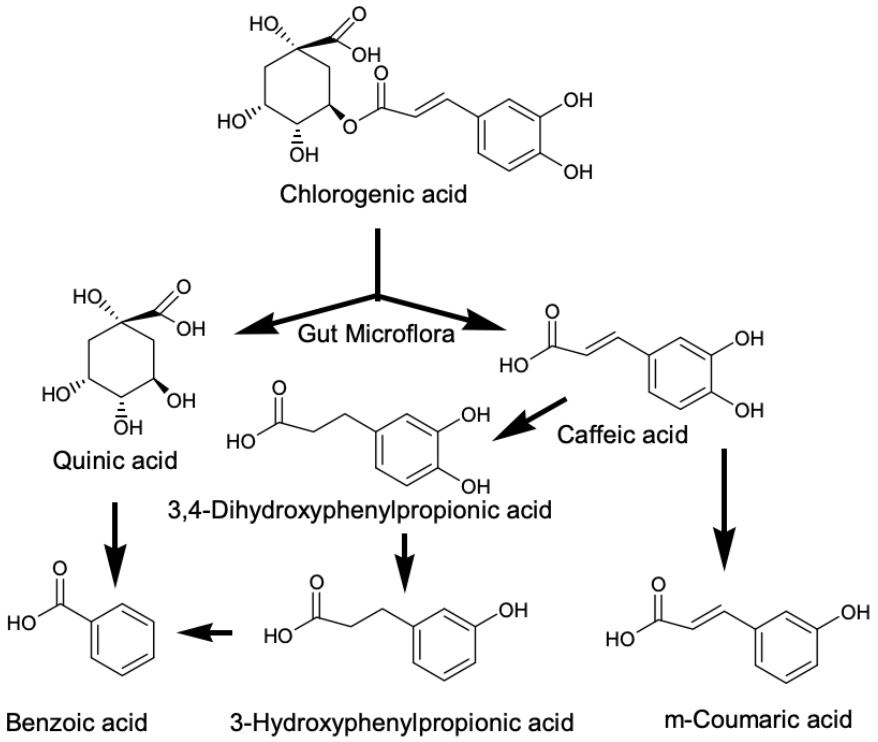

Figure 4. *The pathway of chlorogenic acid metabolism by gut microflora, in which CGA is degraded into quinic acid and caffeic acid and quinic acid is converted into benzoic acid* [24]

2.2 Programmed cell death

Cell proliferation is a vital process among multicellular organisms, in which cells grow and divide continuously throughout cell cycle to replenish dying cells. Meanwhile, cell death is also a vital process of biological cells ceasing to perform their functions. Programmed cell death (PCD) describe any type of cell death, mediated by an intracellular factor [29,30]. A tight regulation of cell proliferation and PCD is fundamental for maintenance of tissue homeostasis. Abnormal in regulation of PCD results in variety of human diseases and cancers. PCD is categorized mainly into apoptosis, necrosis and autophagy; nevertheless, in scope of this thesis, only necrosis and apoptosis which are associated in the regulation of cancer cells are discussed to show interaction between programmed cell death and potential chemotherapeutic agents.

2.2.1 Apoptosis

Apoptosis is the most dominant type of PCD and takes places during the development and aging of normal cells. Apoptosis also serves as defensive mechanism to response cell damage caused by diseases or toxic agents [31,32]. In other words, apoptosis can be triggered by different stimuli; under the same stimulus, only some cells will die to response to it. In specific, anticancer agent, utilized for cancer treatment leads to damage of DNA in several cells, which in turn causes apoptotic death induced via *p53*-dependent pathway. Apoptosis is able to take place in some cells if a ligand binds to TNF receptors expressed on those cells [33,34]. The morphological alternation of apoptotic cells can be observed under light microscopy. At the early stage, apoptotic cells are characterized by cell shrinkage and condensation of chromatin. Subsequently, the size of cells turns into smaller, with condensed cytoplasm, organelles becomes tightly folded [35,36]. Afterwards, budding process takes place, in which blebbing of plasma membrane happens followed by cell fragmentation into apoptotic bodies containing cytoplasm with packed organelles with absence or presence of fragmented nuclear. These apoptotic bodies are enclosed by plasma membrane and then quickly engulfed and phagocytosed by macrophages or by the surrounding cell to avoid inflammation reactions. The alternation of cell morphology undergoing apoptosis is depicted in Figure 5. It is worth pointing out that apoptosis does not cause inflammatory reaction due to the following reasons. Firstly, cellular contents are not able to leak into surrounding environment because they are enclosed by plasma membrane. Secondly, necrosis of apoptotic bodies prevented due to quick digestion of adjacent cells. Lastly, anti-inflammatory cytokines could not be produced by engulfing cells [37,38].

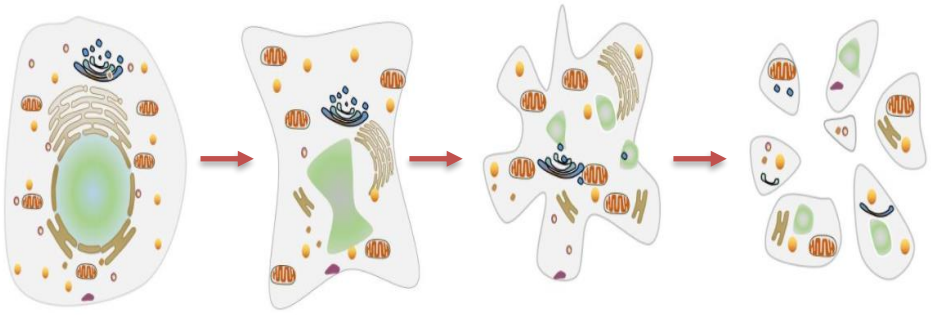

Figure 5. *Morphological alteration of apoptotic cell: cell shrinkage and chromosome condensation. Apoptotic bodies containing organelle and cytoplasm fragment with or without fragmented nuclear* [39]

Apoptosis mechanism is relatively complicated and associated with a cascade of events. Indeed, apoptosis takes place via the extrinsic and intrinsic pathway; however, these

pathways are connected to each other at execution pathway and also have mutual influence [40].

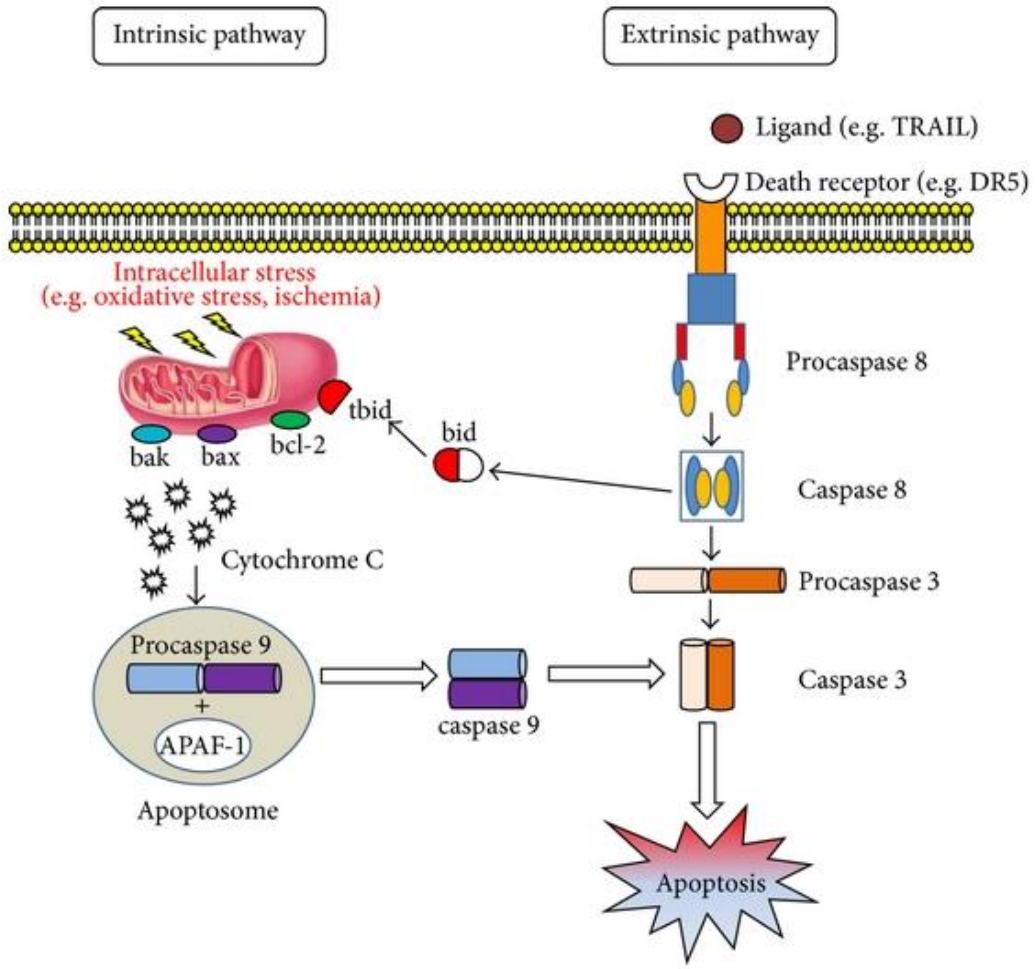

Figure 6. *Two major apoptosis pathways: intrinsic and extrinsic pathway* [41]

As shown in Figure 6, the intrinsic pathway is initiated by intracellular signals produced by non-receptor stimuli. These stimuli could be either positive or negative stimuli. Negative stimuli trigger apoptosis due to the lack of growth factors, hormones and cytokines; meanwhile, positive stimuli are external factors such as radiation, toxins, hypoxia, hyperthermia. Both negative and positive stimuli initiate the alternation in mitochondrial membrane, which in turn trigger opening the pore of mitochondrial permeability transition and liberate two major groups of pro-apoptotic proteins [42]. Cytochrome *c* belongs to the first group of pro-apoptotic proteins and promotes apoptosis by activating caspase-9 [43–45]. In addition, the serine protease HtrA2/Omi triggers apoptosis by impeding the activity of apoptosis protein inhibitors. Besides, AIF, endonuclease G and Caspase-activated DNAse (CAD), which belong to another group of pro-apoptotic proteins, are liberated from the mitochondria during late events of apoptosis. All of these proteins promote DNA

fragmentation into 50–300 kb pieces. Additionally, CAD is also cleavaged by caspase-3 before leading to chromatin condensation [46–48]. It is also worth indicating that Bcl-2 family of proteins works as regulator for apoptotic mitochondrial reactions in intrinsic pathway. Especially, protein *p53* was proven to be involved in regulation of the Bcl-2 family of proteins; nevertheless, the mechanism has not been clarified. Moreover, these proteins are able to promote or hinder apoptosis because they are in charge of mitochondrial membrane permeability. So far, 25 genes encoding Bcl-2 family proteins are discovered. Some of them are anti-apoptotic proteins, preventing apoptosis including Bcl-x, Bcl-XL, Bcl-2; meanwhile, some are called pro-apoptotic proteins, promoting apoptosis which includes Bim, Bik, and Blk.

On the other hand, extrinsic pathway requires the binding of ligand to transmembrane receptors for initiating apoptosis. As such, these death receptors, which belong to tumor necrosis factor (TNF) receptor, are responsible for transmitting the lethal signal from cell surface to the intracellular targets. Up to now, the numerous pairs of ligand and receptor are identified and among them, FasL/FasR as well as TNF-*α*/TNFR1 model are considered as hallmarks for extrinsic pathway of apoptosis. When homologous trimeric ligands in these models bind to their appropriate receptors, cytplasmic adapter proteins with respective death domains will target to receptors. For instance, when homologous trimeric ligand Fas bind to Fas receptor, FADD is recruited and then binds to Fas receptor. After that, FADD connects with procaspase-8 throughout death effector dimerization, in which a signaling complex inducing death is established resulting in procaspase-8 activation and ultimately caspase 3 activation [49,50].

As mentioned in the beginning of this section, these pathways are connected to each other at final execution pathway when execution caspases are activated. All morphological alternations of apoptotic cell such as fragmentation of DNA and apoptotic bodies formation are mainly caused by activation of caspase 3.

2.2.2 Necrosis

In opposition to apoptosis, necrosis as an alternative type of PCD, is a noxious process, in which cell is passive victim of death mode. Therefore, it is also called accidental cell death. Interestingly, apoptosis and necrosis are able to take place simultaneously with the involvement of stimulus, like ATP and caspases [34]. For example, the apoptosis can switch into necrosis due to the low level of intracellular ATP and caspase. In other words, the differentiation between these forms of programed cell death is relatively challenging.

In specific, necrosis triggers cell death in large fields since it is uncontrolled and passive process; while apoptosis as energy-dependent process, causes cell death on individual or groups of cells. In terms of morphological alternation, the cells undergoing necrosis are characterized by swollen cytoplasm, swollen or fragmented mitochondria and organelles, ultimately disrupted cell membrane as depicted in Figure 7. The rupture of cell membrane leads to the release of the cytoplasmic components into intercellular space, which in turn results in the inflammatory reaction [51–53].

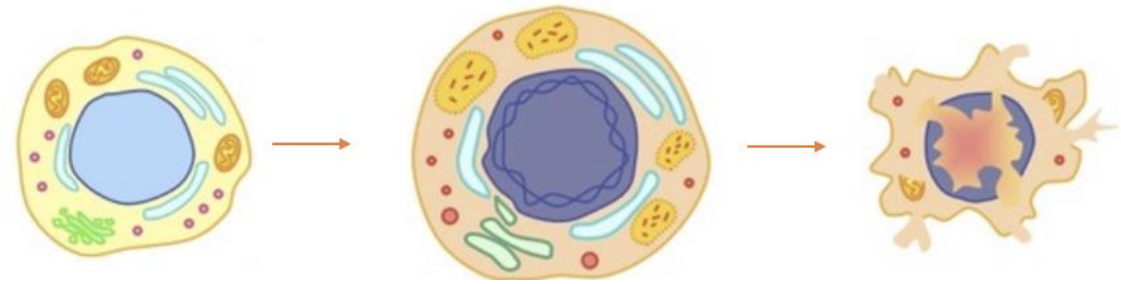

Figure 7. *Morphological alternation of necrotic cell death: swollen cytoplasm, swollen or fragmented mitochondria and organelles, ultimately disrupted cell membrane leads to the liberation of cytoplasmic components and eventually inflammatory reaction* [54]

In terms of mechanism, the necrosis pathway is stimulated by variety of stimuli including bacterial toxin, peritoneal macrophages, immune defense components like cytokines, produced by viruses and bacteria as well as protozoa as illustrated in Figure 8. These stimuli bind to receptors involved in initiating necrosis pathway as TNF, FAS and TRAIL receptors. Especially, cytokines and several other stimuli can promote apoptosis and necrosis pathway. In other words, the switch between these pathways can be adjusted, nevertheless, the outcomes of apoptosis and necrosis are different. Indeed, under stimulation of the receptors, oxidative stress, and DNA damage, stress kinases of JNK and p38 is activated before targeting to proteins of the Bcl-2 family. Besides, DNA damage and excitotoxins can generate necrosis as well. Specifically, binding of excitotoxins to NMDA receptors results in failures in Ca^{2+} homeostasis and in turn cause the change of Ca^{2+}, which are proven to trigger cell death via necrosis. Meanwhile, DNA damage induces necrosis by energy deficiency. All the above stimuli activate the proteases at last stage by caspases resulting in plasma membrane permeabilization as consequence.

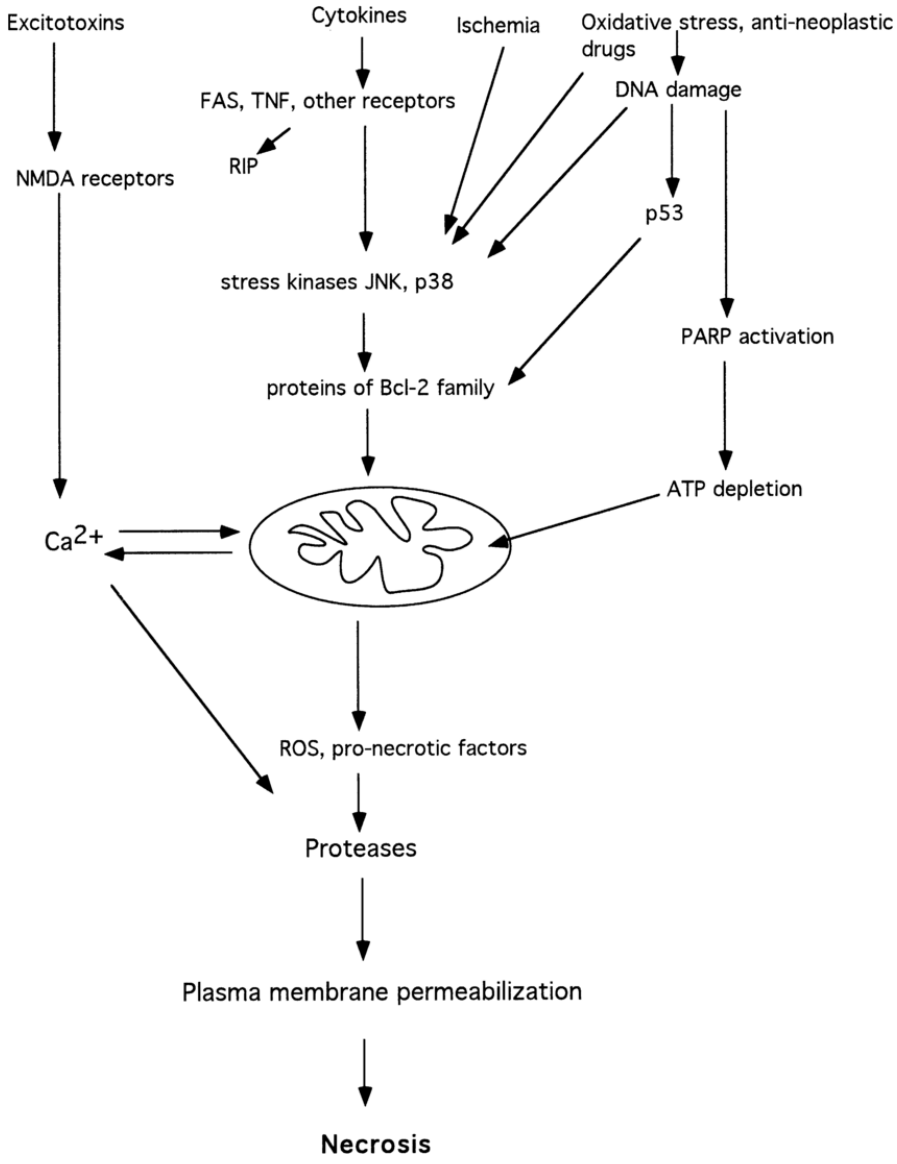

Figure 8. *Illustration of necrosis pathway* [55]

2.3 Statistics and statistical hypothesis test

Statistical hypothesis test is a tool to examine how confident the set of n samples describes properties of a random variable. In this thesis, the focus is on comparing the parameters of two random variables X and Y. Particularly, the mean values of two variables are compared by examining the statistical properties of a set of representatives for each variable. The used statistical test is equal variance t-test (Student's t distribution) with $m + n - 2$ degrees of freedom where m and n are the number of samples taken for each treatment. The results of statistical tests are considered statistically significant if its p-value is smaller than a chosen threshold [56].

3. RESEARCH METHODOLOGY AND MATERIALS

The objective of the work shown in this thesis is to investigate the potential anti-glioblastoma activity of quinic acid derivatives. Therefore, various methods and series of experiments were selected and implemented carefully to ascertain the efficacy of those compounds. The whole experimental approaches are described in this chapter. The image analysis and signal processing as well as statistical techniques are utilized to analyze acquired data from those experiments.

3.1 Materials

The total of 16 quinic acid derivatives (1-16, Table 1) synthesized by Docent. Nuno Rafael Candeias (Tampere University, Tampere, Finland) and characterized for its anti-gliobastoma activity.

Cell lines

The anti-glioblastoma activity of quinic acids derivatives were assessed mainly on two human glioblastoma cell lines (LN229 and SNB19) and mouse embryonic fibroblast cell line (MEF). LN229 and SNB19 were gifted by Dr. Kirsi Granberg (Tampere University, Tampere, Finland) and MEF from Wolfgang H. Ziegler of Hannover Medical School (Hannover, Germany). LN229 expresses mutated p53 tumor suppressor protein from a patient with a glioblastoma multiforme in the right frontal parieto-occipital zone. SNB19 also exhibits p53 mutation from a patient with glioblastoma multiforme, but in the left parieto-occipital zone [57]. MEF provides a preliminary cell model to examine the functions of p53 protein [58,59].

Table 1. *List of synthetic quinic acid derivatives utilized in the studies*

Compound	EPP number	Chemical formula	Molecular weight (g/mol)
1	SHA-82	$C_{10}H_{16}O_7SSi$	308.38
2	SHA-111	$C_{55}H_{66}O_4Si_3$	875.38
3	SHA-150	$C_7H_{12}O_7S$	240.23
4	SHA-159	$C_{46}H_{56}O_7SSi_2$	809.18
5	SHA-161	$C_{53}H_{62}O_9S_2Si_2$	963.36
6	SHA-171	$C_{57}H_{72}O_9S_2Si_3$	1049.57
7	SHA-181	$C_{55}H_{68}O_3Si_3$	861.40
8	SHA-222	$C_{59}H_{78}O_7SSi_4$	1043.67
9	SHA-272	$C_{55}H_{64}O_5Si_3$	889.37
10	AK-4	$C_{39}H_{50}O_5Si_2$	654.99
11	AK-7	$C_{25}H_{52}O_5Si_3$	516.94
12	AK-8	$C_{55}H_{68}O_5Si_3$	893.40
13	AK-15A	$C_{16}H_{36}O_5Si_3$	392.71
14	AK-15B	$C_{16}H_{38}O_5Si_3$	394.73
15	AK-17	$C_{25}H_{56}O_5Si_3$	520.97
16	AK-22	$C_7H_8O_7S$	236.19

3.2 Medium preparation and cell culture

The human glioblastoma cell lines, SNB19 and LN229 and mouse embryonic fibroblast cell line MEF were cultured in Dulbecco's Modified Eagle's Medium (DMEM) which was supplemented with 10% fetal bovine serum (FBS), 1% Penicillin-Streptomycin and 0.025 mg/mL Amphotericin B. These cells were then incubated with proper oxygenation/aeration at 37°C in humidified incubator which maintains at 95% relative humidity and 5% CO_2. These components were purchased from Biowest, St. Riverside, MO, USA and Sigma-Aldrich, St. Louis, MO, USA with codes as shown in Table 2. When the confluence reached to 70%, the cultures were passaged to T75 flasks following standard cell passaging techniques.

Table 2. *Composition of complete medium*

Component	Concentration	Supplier	Supplier Code
DMEM High Glucose	90%	Biowest	L0102-500
FBS	10%	Biowest	S181H-500
Penicillin-Streptomycin	1%	Sigma-Aldrich	P4333
Ampicillin B	0.025 mg/ml	Sigma-Aldrich	A9528

3.3 Sample preparation for the biological assays

Sodium orthovanadate, a tyrosine phosphatases inhibitor, is reported to have antiproliferative effect on human glioblastoma cells and hence, considered as a chemotherapeutic agent for glioblastoma treatment [60]. Additionally, inhibition of cell proliferation, increase in ROS generation and apoptosis on tumor cells, with the positive control, Sodium orthovanadate were also demonstrated [46,61].

In order to acquire a final concentration of 100 mM, the Sodium orthovanadate and each quinic acid derivative were dissolved in DMSO (0.1 %) [15]. The amount of needed DMSO was calculated as following (1)

$$C_M = \frac{m}{M\ x\ V} \qquad (1)$$

In which,

- C_M denotes molar concentration (M)
- m denotes compound mass (g)
- M denotes molecular weight (g/mol)
- V denotes volume (L)

The intermediate dilutions were prepared by diluting 100 mM solution in MQ water (4000 µM and 2000 µM) and final concentrations (100, 75, 50, 25, 10 µM) were diluted by the complete culture medium.

3.4 Cytotoxicity assay by Trypan Blue Exclusion method

In vitro cytotoxicity is defined as the potential of a compound to trigger cell death, one of the most crucial indicators for biological assessment. There are two mode of programmed cell deaths including necrosis and apoptosis. Cellular necrosis represents *in vitro* cytotoxicity in most cases. However, it is worth pointing out that in cancer related cytotoxicity, it is extremely valuable to distinguish apoptosis from necrosis [62]. Therefore, cell cytotoxicity and viability assays are conducted in order to determine cell deaths triggered by these damages.

Cell cytotoxicity and viability assays are commonly utilized in fundamental research and drug screening, especially anticancer agents. The Trypan Blue dye exclusion test is performed extensively for detection of cell viability by staining death cells. The fundamental principle of this method is that Trypan Blue, a polar dye, is not able to enter the viable cells with intact cell membranes, while this polar dye is able to go inside of dead cells with porous membranes, then penetrate and stain the cytoplasm blue [63]. The color difference between stained and unstained cells facilities the quantifying viable cell and non-viable cell populations upon analysis by Countess II FL Hemacytometer (ThermoFisher Scientific, A25750). This correlates to the cytotoxicity and inhibitory effects which the drugs possess on the cell populations.

Depending upon the study, the treated cells were harvested after either 24 h, 48 h, or 72 h treatment time. The cells were trypsinized by adding 350 µL Trypsin-EDTA (T3924-100mL, Sigma-Aldrich, St. Louis, MO) to each well in order to detach adherent cells. The trypsinization was stopped by adding pre-warmed complete culture medium with equal amount of added Trypsin (350 µL) into each well and then centrifuged at 3000 rpm for 10 min to harvest the cells. These cells were resuspended in complete culture medium and Trypan Blue in 1:1 ratio and incubated for 10 min to determine the cell viability. This step was accomplished by quantifying living and dead cells using Countess II FL Hemacytometer.

The assay was carried out with three biological and two technical repeats, and the results were statistically analyzed.

The percentage of cell growth inhibition for each sample were calculated using (2).

$$\text{Inhibition (\%)} = \frac{Mean\ No.\ of\ cells\ in\ DMSO - Mean\ No\ .of\ cells\ in\ treated\ sample}{Mean\ No.of\ cells\ in\ DMSO}\ x\ 100\% \quad (2)$$

In which,

- Mean No. of cells in DMSO represents the mean number of cells in the DMSO control
- Mean No. of number of cells in treated sample represents the mean number of cells in the treated samples.

3.5 Cytotoxicity screening of quinic acid derivatives

Concerning the potential chemotherapeutic drug for glioblastoma, 16 quinic acid compounds were screened to measure the cell growth inhibition potential in glioblastoma. The LN229 cells were seeded at initial density of 1 x10^5 cells per well in 12-well plates. These cells were incubated in humidified incubator (37 °C, 5% CO_2) for 48 hours. When the confluency reached to 70%, the cells were treated with 100 µM of each compound, untreated cells, and DMSO treated as control. After 48 h treatment, cell viability was quantified following the Trypan Blue Exclusion method as described previously. The assay was conducted with a triplicate of each treatment in cell line LN229. The compound, which exhibited the highest percentage of cell viability inhibition, was selected for further dose-dependent cytotoxicity.

The determination of relationship between dose of drug and growth inhibition on cells is important to assess the potency of the chemotherapeutic drug, a key factor in evaluating the effectiveness of the chemotherapeutic drug [64]. Hence, the cell viability assay was implemented to determine this relationship as well as test potency of drug.

Cell lines, LN229 and SNB19 were seeded at density of 1 $x10^5$ cells per well on 12-well plates and maintained at proper culture condition in incubator (37 °C, 5% CO_2). After 48 hours, the cells were treated when it approximately reaches the confluence of 70%. The various concentrations including 25, 50, 75, 100 100 µM of the top leading derivative - AK-4 (from quinic acid derivatives cytotoxicity screening) were utilized to quantify the cell viability. The sodium orthovanadate was used as a positive control and DMSO (0.1%) as a negative control, along with untreated sample. After 48 h exposure, the cells were collected and quantified for live and dead cell percentage by Trypan Blue Exclusion method using Countless II FL Hemacytometer, as described above. The assay was carried out with a triplicate of each treatment in the cell lines, LN229 and SNB19. After obtaining data of viable and non-viable cells, the percentage of cell viability inhibition was calculated by formula (2). Semi-log dose-response curves were generated by Microsoft Excel software using logistic function. In conformity with the dose-dependent curve, the half-maximal inhibitory concentration (IC_{50}) of the top compound for each cell line was calculated.

3.6 Time-dependent cytotoxicity

Time of efficacy is another crucial factor in evaluating the effectiveness of chemotherapeutic drugs. This study is also utilized in determination of therapeutic windows for the drugs. In addition, due to the narrow therapeutic window, the time of efficacy is relatively short for most anticancer drugs. Due to the importance of exposure time, the time-dependent cytotoxicity assay was employed to compare the cytotoxic effect of AK-4 at 24 h, 48 h and 72 h.

Two cell lines, LN229 and SNB19 were seeded at density of 1 $x10^5$ cells per well on 12-well plates and incubated at 37 °C in humidified incubator with 5% CO_2. The cells were treated when confluency was approximately at 70% after 48 hours. The time dependent assay on both the cell lines LN229 and SNB19 were carried out using IC_{50} concentration of AK-4 acquired from dose-dependent cytotoxicity assay for 24 h, 48 h and 72 hours. Sodium orthovanadate and DMSO (0.1%) were used as a positive and negative controls, respectively. Untreated cells were also used as additional control. After each 24 h, 48 h,

and 72 h exposure, the cells were quantified in accordance with the Trypan Blue Exclusion method as presented previously. All the experiments were done in triplicate. After acquiring data of viable and non-viable cells, the percentage of cell viability inhibition after each 24 h, 48 h, and 72 h treatment was calculated also by formula (2).

3.7 Non-cancerous cell line cytotoxicity

The non-selective cytotoxicity of chemotherapeutic drugs exerts cytotoxic effect on both normal and cancerous cells. These effects were considered as the side effects of current chemotherapeutic drugs. The present hypothesis is that quinic acid derivatives may show selectivity between normal as well as cancerous cells, and this hypothesis should be ascertained by experiment.

Hence, in order to investigate whether quinic acid compound – AK-4 performed cytotoxic effects on healthy cells, cell viability assay was employed on mouse embryonic fibroblast MEF cell line. The cells were seeded on 12-well plates with a density of 1 x 10^5 cells per well and incubated until the confluency reached 70% (after 48 hours). The MEF cells were treated with DMSO (0.1%) as negative control, 25 µM and 100 µM AK-4. Untreated cells were also used as additional control. Cell viability was quantified following the Trypan Blue Exclusion method after 48 h exposure. The quantification of living and dead cells was performed using Countess II FL Hemacytometer. The experiment was done in triplicate. The percentage of cell viability inhibition was calculated following the formula (2) to obtain the number of viable and non-viable cells.

3.8 Proliferation scratch assay

Cell migration refers to the integrated multistep process which involves the movement of individual cells or cluster of cells from one site to another site by adopting various motility modes [65]. Cell migration plays a central role in variety of distinct pathologic and physiologic processes such as wound healing, cancer as well as growth and differentiation of cell. The cell migration of normal cells is regulated; nevertheless, the tumor cancer cells are able to move to distant locations and form metastasis. Whereby, the ability to hinder metastasis is one of the most important criteria for an effective chemotherapeutic drug.

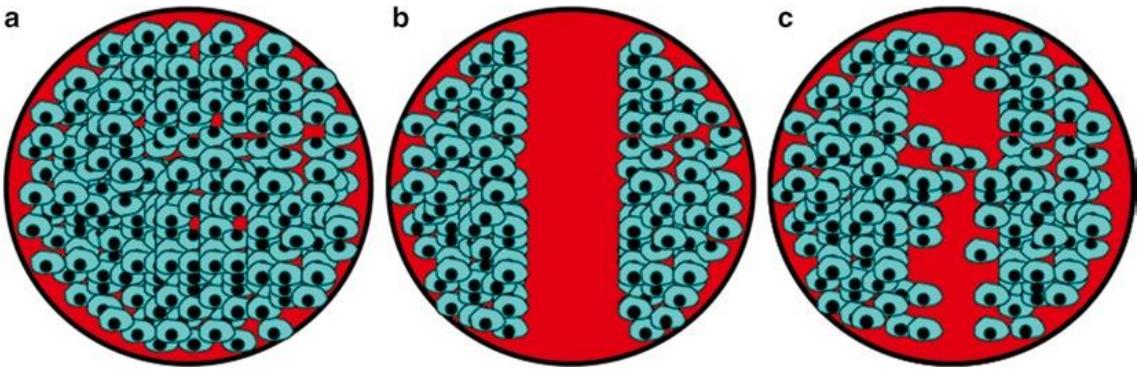

***Figure 9**. Diagram of scratch assay, (a) represents a confluent monolayer of cells, (b) the scratch created on monolayer by using a thin tip and captured as the first image, and (c) the healing of scratch [67].*

Scratch assay is a straightforward and cost-efficiency as well as the simplest assay to assess cell migration *in vitro* (Figure 9). It is based on the observation of scratch, also known as the artificial gap, which is created by a tip or needle across the confluent cell monolayer. Subsequently, the cells at the edges of scratch migrates to cell-free zone created by scratch until this area is completely closed. Briefly, the fundamental steps of scratch assay consist of creating the scratch, capturing images at the beginning and each point of time during cell migration. The image analysis is employed to determine the percentage of cell migration[66].

Glioblastoma multiforme possesses complicated pathogenesis involving mutations as well as alterations of crucial cellular pathways which are related to cell migration and proliferation (allowing for rapid growth) [68]. As such, an effective anticancer drug for glioblastoma should be capable of slowing or halting the glioblastoma multiforme cells migration. Evaluating the effect of AK-4 against the migration of glioblastoma multiforme cells was performed using scratch assay.

In this assay, LN229 and SNB19 were seeded at initial density of 2×10^5 cells/well on 12-well plates, then grown overnight in humidified incubator (37 °C, 5 % CO_2) to obtain a monolayer of adherent cells. The monolayer of cells formed was scratched using 200 µl pipette tip and followed by washing step using 1 ml of the complete culture medium to remove the cell debris and to smoothen the edge of the scratch as well. The IC_{50} concentration of compound AK-4 was mixed with 1 ml of complete culture medium supplemented with 5 % FBS. The untreated cells cultured with complete culture medium sup-

plemented with 5% FBS were prepared as negative control. The scratch area was captured using a light microscope at every 2 h intervals for total of 8 hours. The distance between the edges of scratch at each point of time was measured by image analysis. The scratch closure showed the difference in measurement of scratch width at each point of time (2 h, 4 h, 6 h, and 8 h) with respect to 0 h and the scratch closure percentage was calculated using (3).

$$Scratch\ closure\ (\%) = \frac{Distance\ A - Distance\ B}{Distance\ A}\ x\ 100\% \qquad (3)$$

In which,

- Distance A represents measured distance of the scratch at 0h.
- Distance B represents measured distance of the scratch at 2 h, 4 h, 6 h, and 8 h respectively.

3.9 Detection of Intracellular Reactive Oxygen Species

Reactive Oxygen Species (ROS) are oxygen-containing chemical reactive species. They are reactive molecules and free radicals stemmed from molecular oxygen. It acts as crucial cell signaling when maintained at proper concentration in cells. The state of cellular stress normally causes dramatic imbalance in ROS levels [69].

The release of ROS during electron transport of mitochondrial aerobic respiration is considered as the prime source of ROS. The protective response of cells is initialized to secure their survival when levels of ROS production are low, whereas, an excess of ROS production is implicated in pathogenesis of diverse diseases [70]. Thereby, detection of intracellular ROS production in LN229 and SNB19 cells treated with AK-4 was performed to assess the cellular stress on these cell line.

Variety of methods are available to measure the ROS activity within mammalian cells. The detection of ROS utilizing 2′, 7′-dichlorodihydrofluorescein diacetate (H_2DCFDA) fluorescent probe is widely applied due to its simplicity, fast and affordable cost. The method is based on the principle that the H_2DCFDA is permeable to diffuse passively into the cells which is retained in the intracellular level after cleavage by intracellular esterases. Once the nonfluorescent H_2DCFDA is oxidized by ROS, it is converted to the highly fluorescent 2',7'-dichlorofluorescein (DCF). As such, the fluorescence intensity is proportional to the ROS generation in cell.

LN229 and SNB19 cells were seeded in 12-well plates with the initial density of $1x10^5$ cells per well and grown for 48 hours in incubator at 37 ^{0}C with 5 % CO_2. The cells were dosed with IC_{50} concentration of AK-4 for 5 hours. Subsequently, cells were transferred into 96- well plate after being collected by centrifugation at 3000 rpm for 10 min. Cells were maintained for 30 min with 2 µM H_2DCFDA (Sigma-Aldrich, St. Louis, MO) in incubator at 37 ^{0}C with 5 % CO_2. Afterwards, the cells were washed using pre-warmed PBS and then recovered for 20 min in pre-warmed completed culture medium. The 200 µM concentration of Hydrogen peroxide (H_2O_2, Sigma-Al- drich, St. Louis, MO) was prepared as positive control. The microplate reader (Fluoroskan Ascent FL, Thermo Labsystems) at the wavelength of 485nm excitation and 538nm emission, was used to read fluorescence intensity. The fold increase in ROS generation is calculated using (4).

$$Fold\ increase = \frac{Ftest - Fblank}{Fcontrol - Fblank} \qquad (4)$$

In which,

- F_{test} denotes the fluorescence readings obtained from the treated wells.
- $F_{control}$ denotes the fluorescence readings obtained from the untreated wells.
- F_{blank} denotes the fluorescence readings obtained from the unstained wells.

3.10 Cytotoxicity assay on patient-derived glioblastoma cell lines

Low passage cell lines MMK1 and RN1 from patient-derived primary glioblastomas multiforme cells at low passage, exhibiting the phenotype of glioblastomas multiforme cells, were gifted by Dr. Brett Stringer (Medical Research Institute, QLD, Australia). These cells were isolated from patients' tumor according from Novel Therapies for Brain Cancer, and the approval was obtained from the human ethics committee of the Queensland Institute of Medical Research and Royal Brisbane and Women's Hospital (P3420, HREC/17/QRBW/577) [71].

These cells were seeded at initial density of 10^5 cells/well on 12-well plates with serum-free medium containing 1 % matrigel-coated flasks at 37 °C in incubator supplemented with 5% CO_2 [72]. The cells were then treated with 20 µM concentration of AK-4. The cell viability was quantified following Trypan Blue Exclusion method described above and counted using Countess II FL Hemacytometer after 48 h exposure. The percentage of

cell viability inhibition was calculated following formula (2) after the number of viable and non-viable cells was acquired.

3.11 Statistical data analysis

All results are expressed as mean ± one standard deviation of all biological and technical replicates. Statistical significance was ascertained by equal variance t-tests. The results of statistical tests are considered statistically significant if $p < 0.05$. The result p-value of each test and its degrees of freedom, n will be shown, e.g. p-value = 0.04, n = 4.

4. RESULTS

In this chapter, all the experimental results including raw data, image processing results and statistical evaluation from experiments outlined in chapter 3 were described and examined in detail. This chapter is divided into seven sections. In specific, in the first section, the result from most common method to appraise cytotoxicity of 16 quinic acid derivatives on cell line LN229 is presented. The top compound expressing the highest growth inhibition, is then selected to conduct dose and time - dependent experiments. Afterwards, the next section refers to the inhibitory effect of top compound at different concentrations and time intervals on cell growth of two cell lines LN229 and SNB19 from those experiments. Additionally, the response of healthy cells MEF treated with top compounds is taken into account and thereby, selectivity of this compound toward healthy cells is evaluated utilizing cytotoxicity assay and reported in third section. Subsequently, the top compound is employed to investigate its effectiveness on migration of cell lines LN229 and SNB19; hence, results obtained from these experiments are shown in fourth section. Furthermore, the fifth section mentions ROS generation by cell lines LN229 and SNB19 treated with top compound. Thereafter, the assessment of all modalities of cell death by colony forming assay is demonstrated in the fifth section. Eventually. the induction of cell death by top compound in patient-derived glioblastoma multiforme cell lines MMK1 and RN1 is presented in this last section.

4.1 *In vitro* cytotoxicity of quinic acid derivatives

In fundamental research and drug screening, especially anticancer drugs, cytotoxicity assay is the most prevalent method to assess the preliminary effect of novel compounds. A series of sixteen quinic acid derivatives at 100 µM concentrations were tested for their cytotoxicity activity on glioblastoma cell line LN229. The trypan blue exclusion assay is utilized to examine the cell growth inhibition after 48 h treatment.

The viability of LN229 after treatment with quinic acid derivatives is depicted in Figure 10A. Among sixteen compounds, AK-4 apparently exhibited the highest inhibitory effect on cell line, LN229 at a concentration of 100 µM. Among the sixteen quinic acid derivatives, AK-4 revealed cell growth inhibition of 90.12 % and thus is considered as the most cytotoxic compound in comparison with others. AK-4 compound with the presence of tert-butyldiphenylsilyl (TBDPS) was also represented in Figure 10B .

Other compounds like SHA-161, SHA-181, SHA-159, SHA-171, and AK-8 showed intermediate cytotoxicity like 53.14 %, 48.90 %, 49.99 %, 37.79 % and 30.78 %, respectively. Two other compounds, AK-7 and SHA-82 exhibited low cytotoxicity against LN229, with only 5.54 % and 20.20 %, respectively. Moreover, nearly 100 % of LN229 cells were still viable after treatment with compounds such as SHA-111, AK-17, SHA-150, AK-22, SHA-222, SHA-272, AK-15A and AK-15B.

The statistical tests are conducted in order to verify that AK-4 yields the greatest cytotoxic effect against the growth of LN229, i.e., the calculated p-value is compared with the threshold of 0.05. The comparison of the result from AK-4 and the result from SHA-161, a compound with the second greatest mean value are accessed. The p-value calculated by utilizing function T.DIST.2T is 0.0053 (4 degrees of freedom). Thus, statistically AK-4 yields greater cytotoxic effect than SHA-161. The statistical tests between AK-4 and other compounds were also conducted. All of those tests showed the same outcome as above. Hence, AK-4 exhibits statistically the greatest cell growth inhibition among other compounds.

Thus, AK-4 was the top leading compound with the highest inhibitory effect on cell growth of LN229 compared to other quinic acid derivatives. Therefore, further kinetic studies were carried out using AK-4.

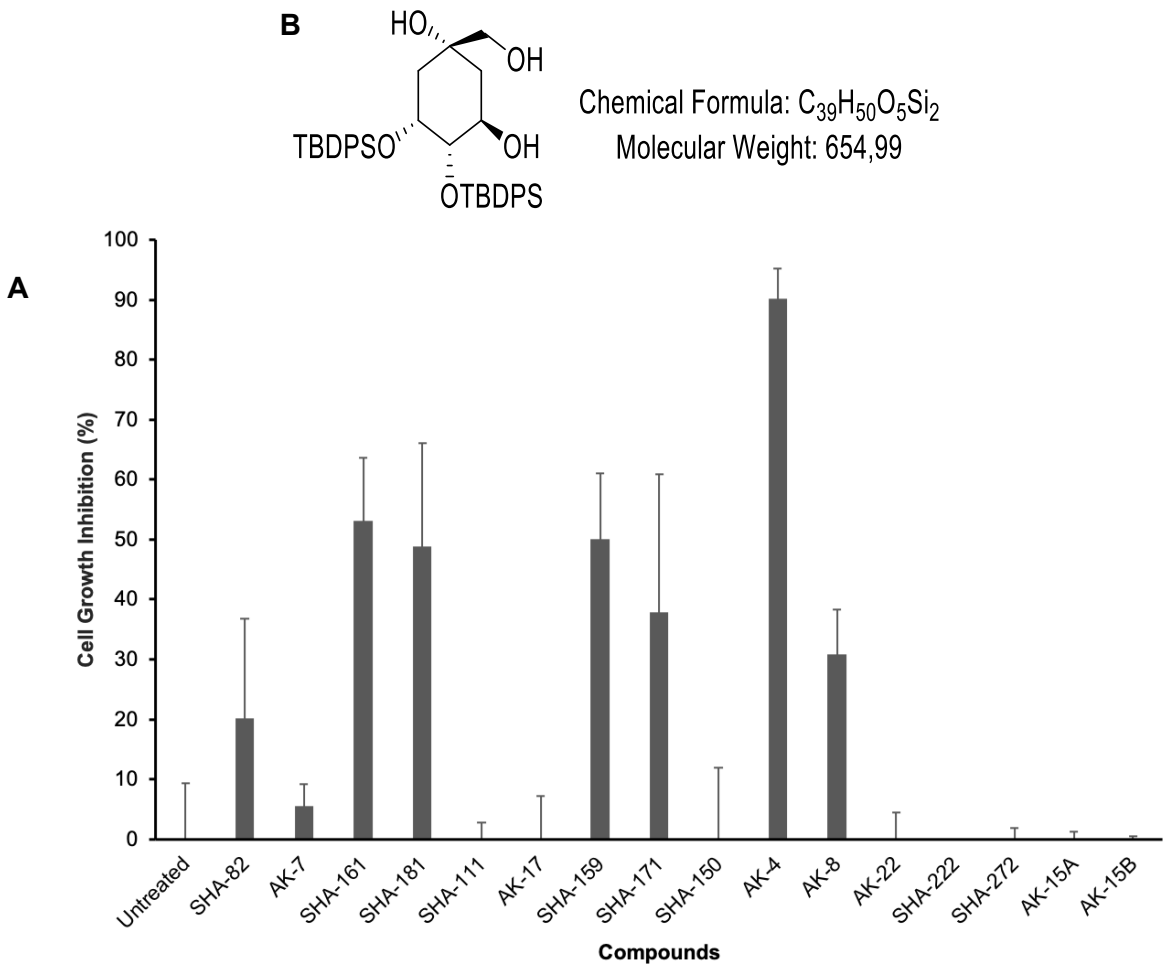

***Figure 10**. (A) In vitro cytotoxicity assays of 16 quinic acid derivatives on LN229 at 100 μM after 48-h drug exposure, in which results are normalized with DMSO control and presented as mean ± standard deviation (n = 3). (B) Chemical structure of AK-4 with tert-butyldiphenylsilyl side group (TBDPS).*

Cell morphology was observed under phase contrast microscope after treatment with AK-4, where a dense monolayer was appeared in untreated cells (Figure 11A); whereas LN229 cells treated with AK-4 were fragmented after 48 h of exposure (Figure 11B).

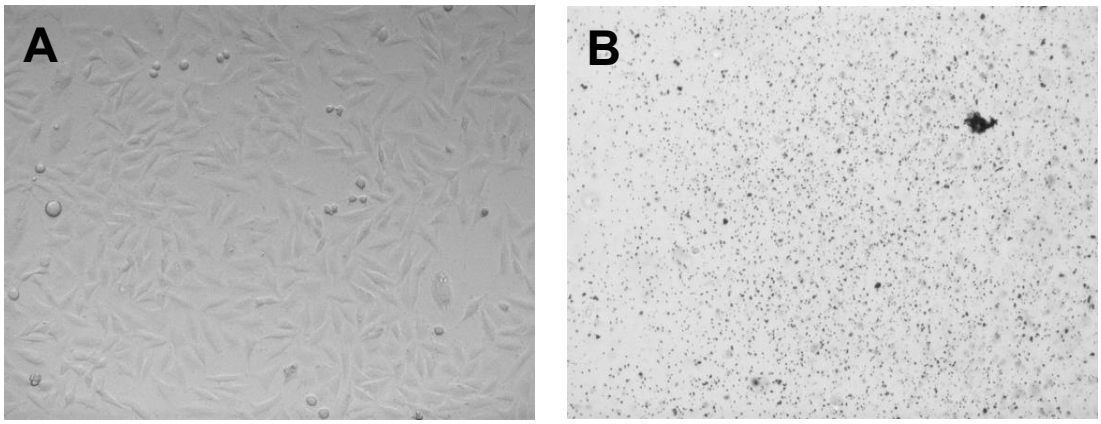

Figure 11. *(A) Images showing the growth of untreated LN229 cells and (B) treatment of LN229 with AK-4 at 100 µM after 48 hours.*

4.2 Induction of cell death by AK-4 in LN229 and SNB19

The top leading compound, AK-4 at four different concentrations of 25, 50, 75, 100 µM were used to conduct dose-dependent pharmacokinetic experiments on both glioblastoma cell lines and the results obtained from the experiments were later plotted as the dose-response curve (Figure 12). Anticancer drugs are most likely to be studied over wide range of doses in preliminary assessment, hence dose-dependent pharmacokinetics have been commonly reported for anticancer drugs than other kind of drugs.

Different concentrations of AK-4 exhibited their inhibitory effects differently against LN229 and SNB19 cell growth. Figure 12 illustrates the change of cell viability percentages on both the cell lines over varying concentrations of AK-4 from 25, 50, 75 and 100 µM. Overall, the inhibitory effect of AK-4 increased over concentrations on both the cell lines. Moreover, the highest cytotoxicity effect of AK-4 was found to be 95.39 ± 1.78 % on cell line SNB19 at 50 µM, whereas AK-4 exhibited the strongest cytotoxic effect against growth of LN229 at 75 µM, in which cytotoxicity was found to be 93.65 ± 2.57 % (Figure 12).

With regard to SNB19, when concentration of AK-4 was increased from 25 to 50 µM, the cytotoxicity raised significantly from 18.15 ± 2.62 % to 95.39 ± 1.78 and reached the highest cytotoxicity at 50 µM. At concentrations of 75 µM and 100 µM, the cytotoxicity effect of AK-4 was found to be approximately 92.36 ± 1.48% and 94.69 ± 2.28 %, respectively.

Meanwhile, cytotoxicity of AK-4 in LN229 was found to be 78.24 ± 6.81 % at 25 µM, which was higher than cytotoxicity of AK-4 in SNB19 at the same concentration. The cytotoxic effect also increased when raising the concentration of AK-4 from 25 to 50 µM; however, the highest inhibitory effect was found to be 93.65 ± 2.57 % at 75 µM. At 100 µM, AK-4 showed decreased growth inhibition, in which cytotoxicity was found to be 92.92 %. As such, the inhibitory effect of AK-4 on LN229 was mostly on par with its effect on SNB19 at 75 and 100 µM concentration of AK-4.

The same statistical test as in section 4.1 is applied, which means that the calculated p-value is compared with the threshold of 0.05. In LN229, the cell growth inhibition exhibited by AK-4 at a concentration of 25 µM is statistically higher than the concentration of 0 µM (p-value of 0.0001, n = 4) and AK-4 at a concentration of 75 µM is statistically higher than the concentration of 50 µM (p-value = 0.0478, n = 4). While the cell growth inhibition is not statistically different between concentration of 25 and 50 µM (p-value = 0.1258, n = 4) or 75 and 100 µM (p-value = 0.8439, n = 4). Thus, it implies that increasing the concentration of AK-4 from 25 to 50 µM or 75 to 100 µM cannot guarantee the increase in cytotoxicity effect. In SNB19, there is statistically significant increase in cell grow inhibition when AK-4 concentration is increased from 0 to 25 µM (p-value of 0.0070, n = 4) or 25 to 50 µM (p-value < 0.0001, n = 4). At the concentration of 50 µM, there is no statistically improvement in cytotoxicity effect against cell growth when increasing the concentration of AK-4 (p-value > 0.05, n =4).

As expected, AK-4 inhibited considerably the growth of both the cell lines and thereby its potential anticancer ability was analyzed further in the following experiments.

The IC_{50} value is the concentration of drug which inhibits viability of cells by 50% and extrapolated from dose-response curve. Sodium orthovanadate with IC_{50} of 50 µM was utilized as control chemotherapeutic drug on both cell lines LN229 and SNB19. IC_{50} values of AK-4 against glioblastoma cell lines were determined by plotting data points over a concentration range of 25 to 100 µM and calculated using regression analysis.

AK-4 revealed IC_{50} values at 10.66 ± 4.71 µM and 28.22 ± 9.87 µM for LN229 and SNB19 respectively. These values were significantly lower than sodium orthovanadate. The lower the IC_{50}, the more cytotoxic to the cancer cell lines; in other words, a low IC_{50} indicates that AK-4 is significantly effective with even a small concentration.

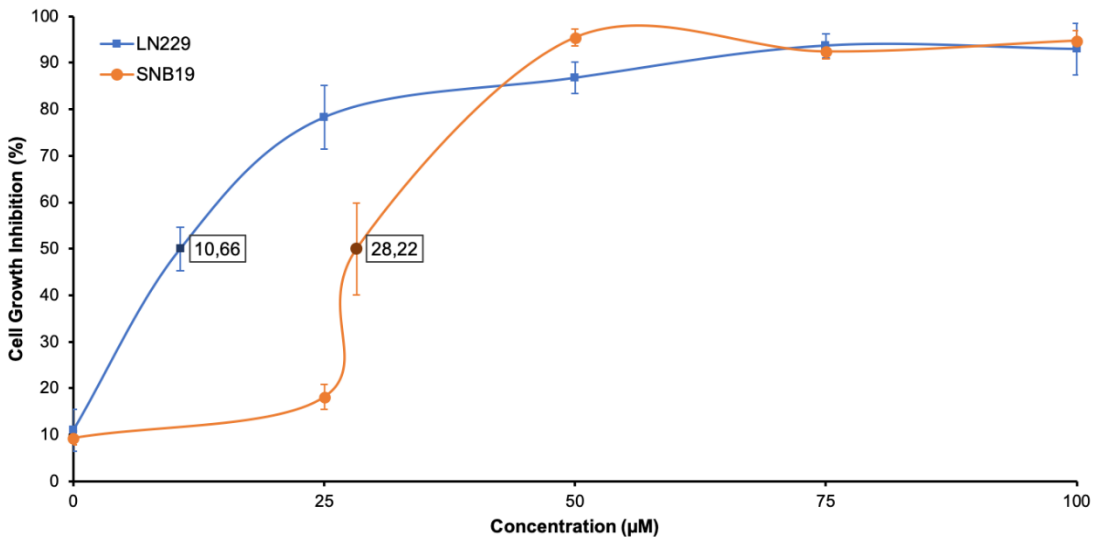

Figure 12. *Dose-dependence cytotoxicity curves used to extrapolate IC_{50} value of AK-4 on both LN229 and SNB19. Where labeled points represent the calculated IC_{50}. The results were normalized with DMSO control and expressed as mean ± standard deviation (n = 3).*

Time of efficacy is also considered as a crucial factor for preliminary assessment of chemotherapeutic drugs. As such, the inhibitory effect on the cell lines LN229 and SNB19 was examined when treated with the IC_{50} concentration of AK-4 after 24, 48 and 72 hours of drug exposure.

In general, AK-4 induced varying cell death on both the cell lines and showed lower cytotoxicity in comparison to sodium orthovanadate over time, as depicted in Figure 13.

In LN229, both AK-4 and sodium orthovanadate revealed a steady increase in cell growth inhibition over time. The percentage of cell death induced by AK-4 was 20.18 % at 24 h and which increased to 32.28 % at 48 h and 38.48% at 72 h of exposure. Likewise, 70 % of cell death was exhibited by sodium orthovanadate at 24 h after which there is gradual increase of cytotoxicity to 90.12 % and 98.85 % at 48 and 72 h exposure, respectively.

Similarly, the cytotoxicity of AK-4 and sodium orthovanadate also increased gradually in SNB19 over time. In SNB19, AK-4 was more competitive with a difference of 27.41 % cell death in comparison with sodium orthovanadate, while this difference in LN229 was 60.37 %. Specifically, AK-4 showed the lowest inhibitory effect against the growth of

SNB19 at 24 h of exposure, in which cytotoxicity was found to be 43.35 %. The cytotoxicity of AK-4 remained relatively stable at 45.74 % at 48 h of exposure before reaching to 53.86 % at 72 h of exposure. Sodium orthovanadate initially exhibited a fairly high cell growth inhibition, in which cytotoxicity was found to be at 57.95 % at 24 h of exposure and increased slightly to 62.22 % at 48 h of exposure. Sodium orthovanadate reached to the highest inhibitory effect against the cell growth of SNB19 at 72 h of exposure, in which cytotoxicity was found to be 81.27 %.

The statistical test is applied to compare the effect of AK-4 with sodium orthovanadate treatment over time. Regarding to LN229, the p-value is 0.0028 (n = 4) when comparing AK-4 with sodium orthovanadate treatment after 24 hours of treatment, which shows that AK-4 has statistically lower inhibitory effect than sodium orthovanadate. The same results occur also at 48 h and 72 h post-treament with p-values as 0.0005 (n = 4) and 0.0020 (n =4), respectively. In the case of SNB19, only after 72 hours of drug exposure, the inhibitory effect of sodium orthovanadate dominates AK-4 with p-value of 0.0072 (n = 4). Otherwise, with the p-value as 0.0850 (n=4) for 24h and 0.0723 (n=4) for 48h post-treatment, statistical method shows that inhibitory effect of AK-4 is not different to sodium orthovanadate.

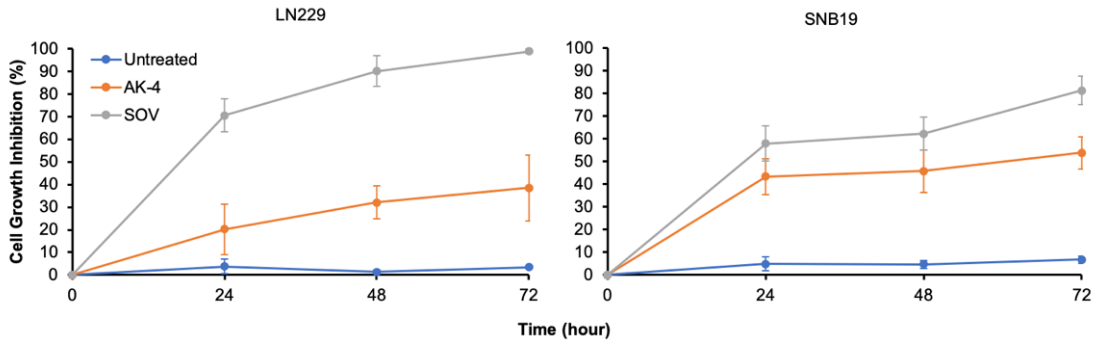

Figure 13. *Time-dependent effect of AK-4 in LN229 and SNB19. All the results were normalized with DMSO control and presented as mean ± standard deviation (n = 3). On LN229, all results are significant between sodium orthovanadate (SOV) and AK-4 (all p < 0.003). On SNB19, only the result at 72 h point is significant between sodium orthovanadate and AK-4 with p = 0.0072. At 24 and 48 h post-treatment, p = 0.085 and 0.072 respectively.*

4.3 Effect of AK-4 in mouse embryonic fibroblast cell line

The therapeutic safety is considered as one of the most crucial concerns when utilizing anticancer drugs to treat cancer patients. Comparing IC_{50} of anticancer drugs can be utilized to examine their safety on cancer cells in comparison with normal cells [73]. But, IC_{50} does not show selectivity towards certain cell types. Therefore, in order to investigate the selectivity of AK-4 to certain cell type, the cytotoxic effect of AK against growth of normal cells was assessed in non-cancerous cell line at concentration of 25 and 100 µM utilizing trypan blue exclusion essay.

In Figure 14, it is observed that AK-4 exhibited high cytotoxic effect in the cell lines including non-cancerous cell line MEF, LN229, SNB19 at 100 µM; however, its effectiveness declined when the concentration was reduced to 25 µM. In specific, at 100 µM AK-4 concentration, the cytotoxicity in MEF was found to be 54.05 %, which was markedly lower than cytotoxicity of AK-4 in both glioblastoma cell lines. At 25 µM concentration, AK-4 showed decreased cytotoxic effect against the growth of cell lines. The cytotoxicity of AK-4 in MEF was found to be 19.98 %, which was significantly lower than cytotoxicity in LN229 (78.24 %); whereas, it was slightly higher than in SNB19 (18.15 %) at the same concentration.

Statistical test is also used to examine the mean value of cell growth inhibition between MEF and glioblastoma cells. MEF cells treated with AK-4 at a concentration of 100 µM yields the statistically lower cytotoxic effect than LN229 (p-value = 0.0031, n = 4) and SNB19 (p-value = 0.0035, n =4), which were treated with AK-4 at the same concentration. While at a concentration of 25 µM, AK-4 showed statistically comparable cytotoxic effect in MEF and SNB19 (p-value = 0.6929, n = 4); whereas, the cytotoxicity of AK-4 in MEF is statistically lower than LN229 (p-value = 0.0005, n = 4). The result is shown in Figure 14.

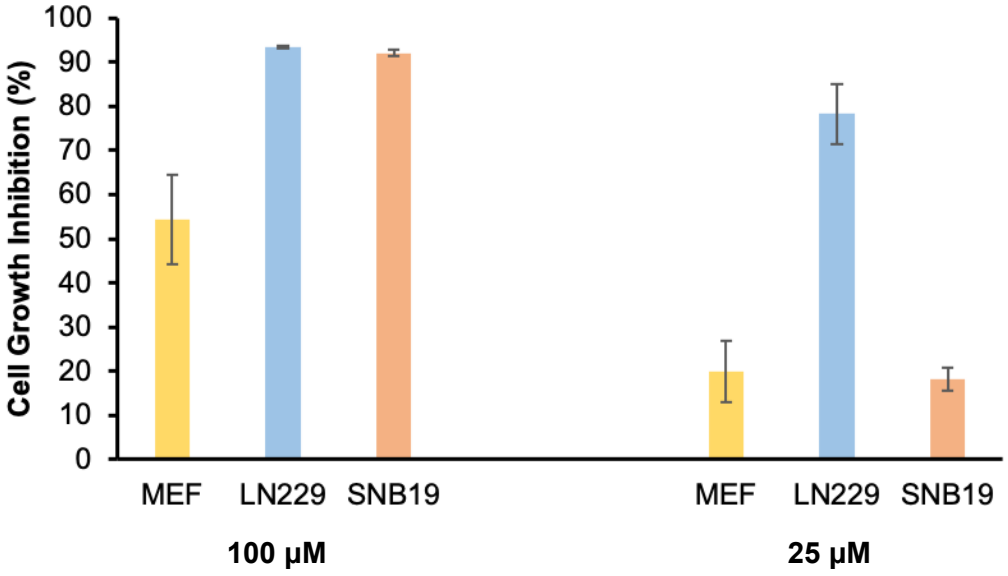

Figure 14. *Cytotoxicity assay in MEF at 25 and 100 µM concentration of AK-4 in comparison to LN229 and SNB19 cytotoxicity at the same concentrations. All the results were normalized with DMSO control and expressed as mean ± standard deviation (n = 3). LN229 100 µM, p = 0.003; SNB19 100 µM, p = 0.004; LN229 25 µM, p < 0.001 and SNB19 25 µM, p = 0.693.*

4.4 Effect of AK-4 against the migration of glioblastoma multiforme cell lines

Cancer metastasis is a major cause of cancer death, which occupies approximately 90 % of cancer death, not primary tumors [74]. Metastasis involves multiple steps including detachment from primary tumor, migration, invasion to different locations and adhesion for growing [75]. In another words, cell migration is considered as one of the most crucial characteristics of cancer. Therefore, the potential chemotherapeutic drugs should be able to hinder the migration of cancer cells. Likewise, inhibitory effect of AK-4 at IC_{50} concentration against the migration of glioblastoma cell lines was evaluated as well.

A variety of methods such as chamber assay or barrier assays are utilized for visualizing the cell migration; however, these methods are not cost-effective, while scratch assay is

a simple and cost-effective method. Whereby, the scratch assay was performed to test inhibitory effect of AK-4 against the migration of both the cell lines. At appropriate culture conditions, the adherent cells grow and create a confluent cell monolayer on the surface. Under mechanical stresses; for instance, a scratch, these cells response by releasing rapidly growth factors which enhance cell migration. Cell migratione can be quantified by time-lapsing photography with microscope at time intervals. The inhibitory effect of AK-4 against the migration of glioblastoma cell lines was measured at every 2 h intervals for total 8 of hours by using light microscope to capture photomicrographs (Appendix A.1 and A.2). The migration of cells treated with sodium orthovanadate at a concentration of 50 µM was also used as positive control.

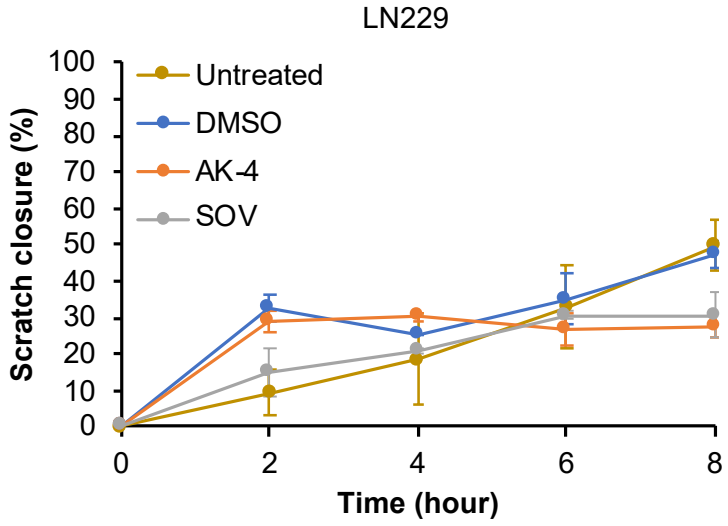

***Figure 15**. Quantification of scratch closure in LN229, in which all data points represent mean ± standard deviation (n= 4 for AK-4 and n = 2 for others).*

As illustrated in Figure 15, it can be seen that the scratch closure percentage of LN229 treated with AK-4 and sodium orthovanadate was inhibited significantly at 8 h post-treatment in comparison with negative controls. Sodium orthovanadate, DMSO-treated cells and untreated cells exhibited increased the scratch closure percentage. The scratch closure percentage of cells treated with AK-4, on the other hand, remained relatively stable over 8 hours of exposure.

Looking in more detail, the scratch closure percentage of cells treated with AK-4 was found to be 28.80 % at 2 h, which was higher than the untreated cells and sodium orthovanadate-treated cells at the same time and increased slowly to 30.10 % at 4 h. AK-4 showed inhibitory effect against the migration of LN229 at 6 h and 8 h of exposure, in which scratched area percentage was found to be 26.50 % and 27.60 %, respectively.

These values were lower than percentage of scratch closure in both positive and negative controls at same time.

In terms of sodium orthovanadate, the scratch closure percentage increased steadily for first six hours until it reached a plateau at 8h. In specific, percentage of scratch closure was found to be 15.30 %, 20.50 %, 30.80 %, and 30.7 % at 2 h, 4 h, 6 h and 8 h respectively.

Interestingly, untreated and DMSO treatment followed a very different trend from 2 to 6 h. The scratch closure percentage of untreated cells was found to be 9.3 % at 2 h and 18.6 % at 4 h and 33 % at 6 h, while the scratch closure percentage of DMSO-treated cells was found to be 32.50 %, 25 %, and 35 % respectively. At 8 h, the scratch closure percentage of untreated and DMSO treatment was 49.8 % and 47.5 %, respectively.

Accordingly, at 8 h post-treatment, the figure demonstrates that AK-4 exhibited a similar inhibitory effect on migration of LN229 compared to sodium orthovanadate. Additionally, AK-4 showed considerable reduction in migration of LN229 cells relative to negative controls.

The same statistical test to compare the mean values of results from AK-4 and other treatments in LN229 as mentioned in previous sections is applied. However, in this experiment, the scratch closure in AK-4 treatment was measured in quadruplicates for each corresponding time point, while the scratch closure in other treatments were measured twice. At 2 h of exposure, AK-4 treatment possesses the scratch closure percentage statistically higher than untreated ($p = 0.0047$, $n = 4$) and sodium orthovanadate treatment ($p = 0.0204$, $n = 4$), while it is statistically equal to DMSO treatment ($p = 0.2353$, $n = 4$). At 4 h of exposure, the result only keeps when comparing with sodium orthovanadate treatment ($p = 0.0012$, $n = 4$), while the scratch closure percentage in AK-4 treatment is higher than DMSO ($p = 0.0176$, $n = 4$) and statistically equal to untreated ($p = 0.0990$, $n = 4$). At 6 h post-treatment, the result from AK-4 treatment is statistically equal to all treatments ($p = 0.3300$ for untreated, $p = 0.1326$ for DMSO, $p = 0.2667$ for sodium orthovanadate, $n = 4$ for all treatments). Finally, the scratch closure percentage in AK-4 treatment is statistically lower than both untreated ($p = 0.0043$, $n = 4$) and DMSO ($p = 0.0024$, $n = 4$) treatment, while it is statistically equal to the one from sodium orthovanadate at 8 h post-treatment ($p = 0.4400$, $n = 4$).

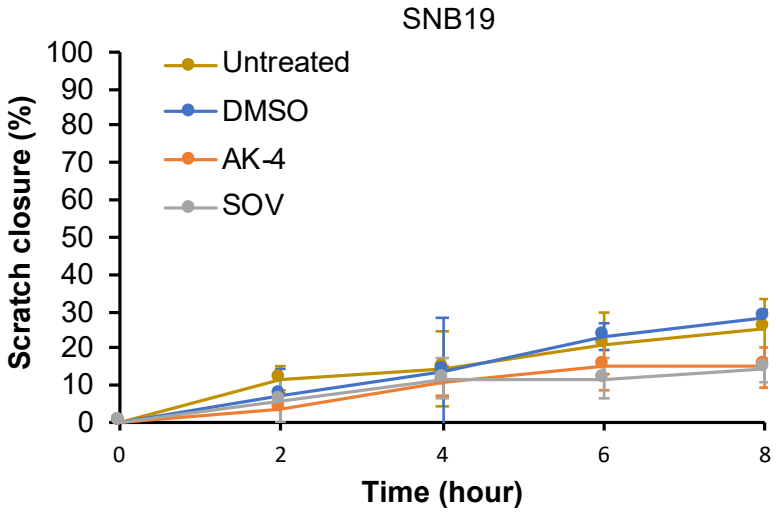

Figure 16. *Quantification of scratch closure in SNB19, in which all data points represent mean ± standard deviation (n = 3 for SOV and n = 4 for others).*

The Figure 16 depicts a slight rise in the scratch closure percentage in SNB19 over the time. Likewise, both AK-4 and sodium orthovanadate exhibited inhibitory effect against the migration of SNB19 but at moderated level.

In specific, it can be observed that the scratch closure percentage was found to be 3.60 % at 2 h post-treatment and increased gradually to 11.30 % at 4 h of exposure. AK-4 exhibited inhibitory effect against the migration of SNB19, in which scratch closure percentage was found to be 15.10 % at 6 h and maintained at 15 % at 8 h post-treatment.

The scratch area percentage in sodium orthovanadate treatment was found to be 5.9 % at 2 h, after which it increased gradually to 12 % at 4 h before staying constant for two following hours and ultimately increased scratched area percentage to 14.2 % at 8 h of exposure. In other words, treatment with sodium orthovanadate expressed similar inhibitory effect on the migration of SNB19 compared to treatment with AK-4 at two points of time, 4 h and 8 h.

With regards to negative controls, as expected, their scratch area percentage was generally higher than treatments with AK-4 and sodium orthovanadate over time. Specifically, scratch closure percentage in untreated cells was found to be 11.80 % at 2 h post-treatment, while the respective value from DMSO-treated cells was 7.1 %**.** At 4 h of exposure, the scratch area percentage of untreated cells and DMSO-treated cells reached

to 14.30 % and 13.70 %, respectively. The scratch area percentage of untreated cells continued to increase from 21.40 % at 6 h to 25.20 % at 8 h compared to 23.30 % at 6 h and 28.60 % at 8 h of exposure for treatment with DMSO.

Consequently, it is apparent that the migration of SNB19 was inhibited by AK-4 and sodium orthovanadate, which exhibited lower scratch closure percentage over 8 h post-treatment relative to negative controls.

The same statistical test is also applied to compare the mean values of result from AK-4 and other treatments in SNB19. Nevertheless, in this experiment, the scratch closure in sodium orthovanadate treatment was measured in triplicates for each corresponding time point, while the scratch closure in other treatments were measured in quadruplicates. After 2 h of treatment, the scratch closure percentage in AK-4 treatment is statistically equal to all other treatments ($p = 0.1197$, 0.5968 and 0.6857 for untreated, DMSO and sodium orthovanadate treatment, respectively with $n = 3$ for all). The same result is obtained at 4 h of treatment ($p = 0.6049$, $n = 6$ for untreated, $p = 0.7579$, $n = 6$ for DMSO, $p = 0.8534$, $n = 5$ for sodium orthovanadate), at 6h ($p = 0.2787$, $n= 6$ for untreated, $p = 0.0674$, $n =6$ for DMSO, $p = 0.5283$, $n = 5$ for sodium orthovanadate), and at 8h ($p = 0.0898$, $n = 6$ for untreated, $p = 0.8337$, $n = 5$ for sodium orthovanadate) with the exception that the scratch closure percentage in AK-4 treatment is statistically lower than the treatment of DMSO after 8 hours of treatment ($p = 0.0035$, $n = 6$).

It is also worth pointing out that both the cell lines treated with AK-4 started detaching from plate at 8 h of exposure.

In conclusion, AK-4 was effective against the migration of both glioblastoma cell lines, especially in LN229. Furthermore, the effectiveness of drug was dependent to the drug exposure time.

4.5 ROS generation by glioblastoma multiforme cell lines treated with AK-4

The elevated reactive oxygen species (ROS) level has been detected in almost cancers and could be considered as the prevalent hallmark of cancer progression . Nevertheless, the cancer cells also perform the detoxification from ROS by surging level of antioxidant proteins [76,77]. This indicates that the function of cancer cells requires a balance of

intracellular ROS production as well. The high ROS level is capable of damaging proteins, nucleic acids and resulting to the activation of intrinsic apoptosis pathway [78]. As such, ROS generation is one of evaluation criteria in screening novel chemotherapeutic drugs. The ROS assay was carried out to investigate the ROS mediated apoptosis in glioblastoma cells treated with IC_{50} concentration of AK-4, utilizing 200 µM H_2O_2 as positive control.

The level of ROS is directly proportional to fluorescence intensity yielded by H_2DCFDA. As illustrated in Figure 17, ROS generation was promoted considerably by AK-4 in both glioblastoma cell lines. It is explicitly observed that, AK-4 treatment elevated a notable fold change of ROS in LN229 with 2.9-fold increase, whereas, only with 1.1-fold in SNB19. This demonstrated that AK-4 was effective in enhancing the ROS production in both LN229 and SNB19. Yet the noticeable difference of 1.8-fold increase between ROS level in both the cell lines indicated that higher ROS level was triggered by AK-4 in LN229. On other words, AK-4 became more effective in elevating ROS level in LN229 than in SNB19. Furthermore, the elevated ROS generation of LN229 cells treated with AK-4 was found to be equal to H_2O_2 control. With regards to SNB19, the ROS production promoted by AK-4 was just under level of ROS in H_2O_2 control, which was 1.4-fold increase. It is suggested that AK-4 exhibited equivalent effect on promoting ROS level in comparison with H_2O_2 control.

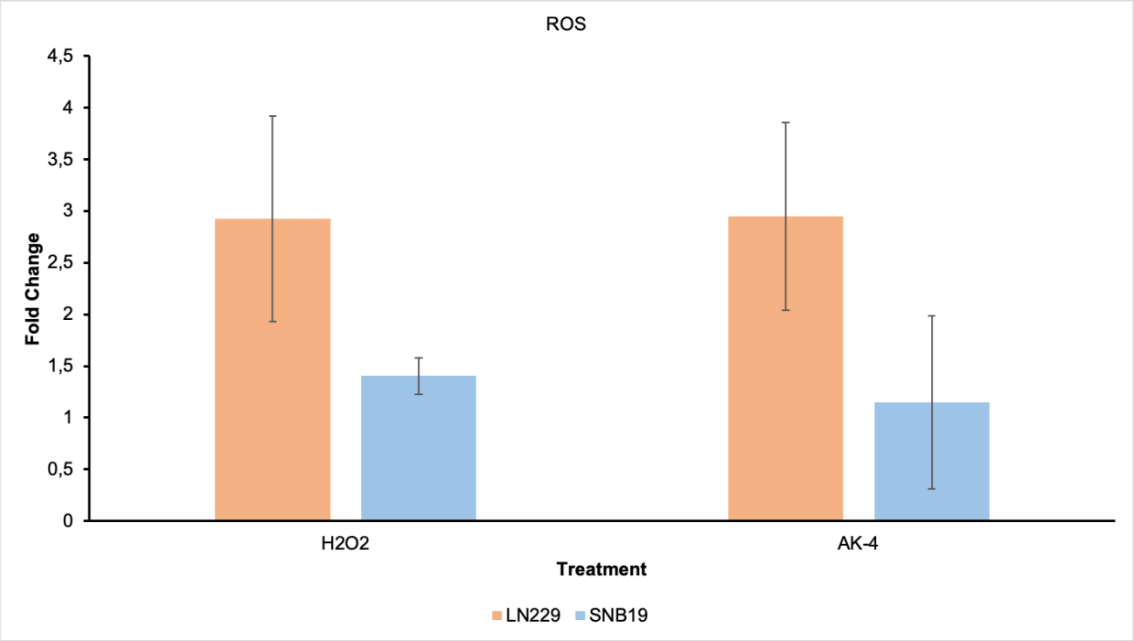

Figure 17. *Elevated intracellular ROS level in LN229 and SNB19, which were treated with IC_{50} concentration of AK-4. The 2 µM H_2DCFD as fluorescent probe, was used to determine fluorescence intensity and 200 µM H_2O_2 was utilized as positive control. All the results were expressed as mean ± standard deviation (n = 3).*

The statistical test is made to confirm the afore mentioned results. First, the change of ROS in LN229 is compared with the one in SNB19 under AK-4 treatment. It is shown that the treatment is indeed more effective in LN229 with p-value of 0.0438 (n = 5). When comparing effectiveness of AK-4 with H_2O_2, it is shown that they are statistically comparable with p-value of 0.9734 for LN229 (n = 6) and 0.5666 (n = 5) for SNB19 cell lines.

The cytotoxicity of AK-4 was again verified in ROS assay, where an elevated amount of ROS, associated to activation of intrinsic apoptosis pathway, was produced by AK-4 in both glioblastoma cell lines.

4.6 Induction of cell death by AK-4 in patient-derived glioblastoma cell lines RN1 and MMK1

Low passage, serum free cell lines as RN1 and MMK1, cultured from patient-derived primary glioblastoma multiforme (GBM) cells has been considered as the benchmark for preclinical studies as well as research on glioblastoma biology [79]. Thus, the efficacy of AK-4 for GBM treatment was examined by conducting cytotoxicity assay on RN1 and MMK1.

In Figure 18, the growth of both RN1 and MMK1 was considerably inhibited by AK-4 at a concentration of 20 μM. The percentage of cell growth inhibition in RN1 was found to be 91.33 ± 5.36 %, while percentage of cell growth inhibition in MMK1 was 88.31 ± 3.63 %. Those results are statistically comparable with p-value of 0.4644 (n = 4). These demonstrated that AK-4 was a promising chemotherapeutic agent for GBM treatment.

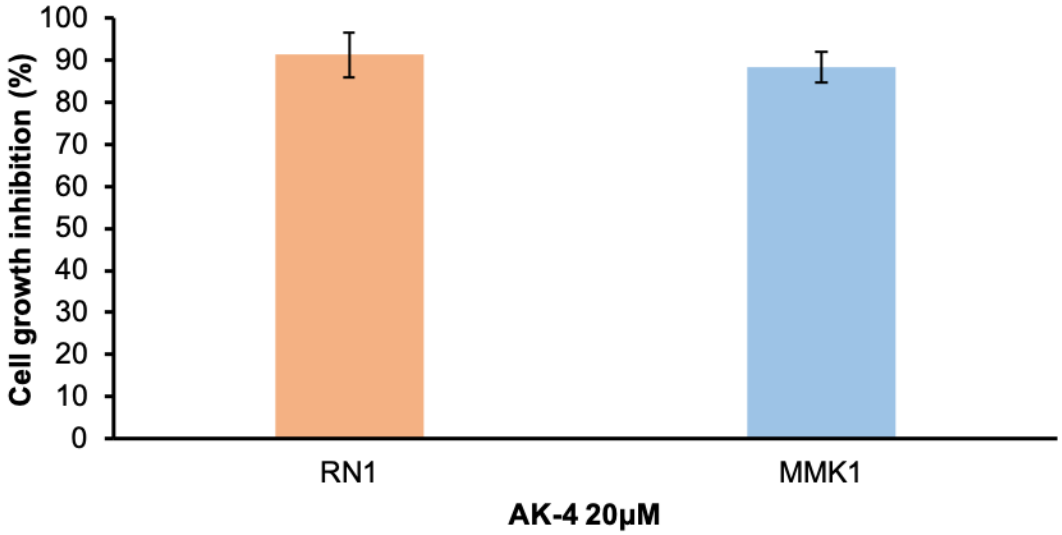

Figure 18. *The cytotoxicity effect of AK-4 on cell lines RN1 and MMK1 at 48 h post-treatment. The results were normalized with DMSO control and presented as mean ± standard deviation (n = 3).*

5. DISCUSSION

The aim of this chapter is to critically examine acquired results in chapter 4 in the light of previous state of chemotherapeutic agents screening methods as outlined in the background and in previous studies. The promising anti-tumor activity of quinic acid derivatives is also demonstrated in this chapter and consequently, may contribute new insights for further studies about chemotherapy for treating glioblastoma multiforme. The possible limitations during research process are acknowledged as well to provide an accurate picture of what can and cannot be concluded from this study; afterwards, options for eliminating such limitations are presented. Eventually, suggestions for further studies to elevate the practical applications of this work are mentioned.

In recognition of natural quinic acid as potential chemotherapeutic agent with strong ability of antioxidative, anti-inflammatory, and anticancer properties, chemical synthesis of quinic acid derivatives is becoming more prevalent for various cancers and diseases treatment. The synthesis of derivatives, derived from quinic acid, can be approached by different manners such as molecular rearrangement, attachment or substitution of functional groups [80,81]. Nevertheless, there is not much evidence to prove efficacy of quinic acid derivatives on glioblastoma multiforme.

The paramount objective of this study was to investigate the potential anticancer characteristics of sixteen quinic acid derivatives against the growth of GBM. This objective was achieved by the following findings, which generated important insights into the role of quinic acid derivatives in chemotherapy and aided their preclinical biopharmaceutics as well as pharmacokinetic studies.

After screening of sixteen quinic acid derivatives, it is found that compound AK-4 exhibited the highest inhibitory effect against the growth of GBM cells with respect to others. As proven [82], the presence of highly reactive tert-butyldimethylsilyl group, not only plays a crucial role for protecting group from organic synthesis and but also enhances the cellular uptake of drugs toward cancer cells by introducing lipophilicity in drugs. As such, it is hypothesized that the presence of tert-butyldiphenylsilyl, which belongs to silyl group as well, enhanced significantly the cytotoxicity of AK-4 compound; however, further studies are required to verify this hypothesis.

Herein the low concentration of AK-4 was adequate to induce high growth inhibition of glioblastoma cells. Anti-glioblastoma inhibitory potency (IC_{50}) was calculated to be 10.6 and 28.2 μM in LN229 and SNB19 respectively, while IC_{50} values of Temozolomide (TMZ), the known chemotherapeutic agent approved by United States of America - The Food and Drug Administration (FDA) in 2005 for GBM treatment, were determined at 75.4 μM in LN229 and 84.4 μM in SNB19 [57,83]. The IC_{50} values of AK-4 in both the cell lines are much lower than those of TMZ with the remarkable difference of 64.8 and 56.2 μM in LN229 and SNB19 respectively. In other words, since AK-4 shows higher inhibitory effect toward growth of both the cell lines than TMZ, this implies that AK-4 could be a potential novel anticancer agent. This implication is in agreement with many studies demonstrating the cytotoxic capability of quinic acid derivatives on breast, liver and lung cancer cells [17,84]. However, further examinations are required to corroborate this because cell death may be induced by various factors as well as complicated mechanisms.

It is worth pointing out that increasing the dose of AK-4 from 25 to 50 μM or 75 to 100 μM cannot guarantee the increase in growth inhibition of LN229 since there is not statistical difference between those values. In contrast, there is statistically improvement in cytotoxic effect of AK-4 in SNB19 when the dose is increased from 25 to 50 μM. From concentration of 50 μM, there is no statistically improvement in growth inhibition of SNB19 when increasing the dose of AK-4 to 75 or 100 μM.

Previously, quinic acid derivatives including 5-caffeoy1 quinic acid and 4-caffeoy1 quinic acid were studied simultaneously on breast cancer cell line, which showed cytotoxic effect to breast cancer cells without harmfulness to non-cancerous cells [25]. This thesis suggests a similar finding that AK-4 showed considerably lower cytotoxicity in MEF than two glioblastoma cell lines, with exception of AK-4 treatment at 25 μM in SNB19. As depicted by dose-dependent curve in Figure 12, this could be understood that at a concentration of 25 μM, the cytotoxicity of AK-4 has not increased exponentially and the difference of cell growth inhibition between MEF and SNB19 is relatively small; therefore it is not able to conclude clearly that cytotoxicity of AK-4 towards MEF is higher than SNB19 at 25 μM. It is believed that with additional targeting, AK-4 could achieve the cytotoxic threshold with minimal effect on non-cancerous cells and turn out to be more selective towards cancer cells.

Furthermore, the application of patient-derived glioblastoma cell lines in preclinical cancer research is becoming prevalent because such cell lines are able to preserve genetic

diversity as well as fidelity of human glioblastoma multiforme [85]. In this study, two patient-derived glioblastoma cell lines MMK1 and RN1 were utilized to assess cytotoxicity of AK-4 toward these cell lines. It is observed that at a concentration of 20 μM AK-4 induced considerably cell death by around 90 % in both MMK1 and RN1. This outcome demonstrates strong inhibitory capability of AK-4 towards patient-derived glioblastoma cell lines in comparison with Temozolomide, a control chemotherapeutic agent, which exhibited approximately 20 % growth inhibition on these cell lines in afore study at a concentration of 100 μM [57]. This implies that AK-4 is a potential chemotherapeutic agent for patient-derived glioblastoma cell lines.

The time-dependent effect of AK-4 on the growth inhibition of glioblastoma also revealed significant outcomes. The increase of inhibitory effect against the growth of glioblastoma cell lines could be achieved by increasing the intracellular concentrations of AK-4 over the time. Moreover, the AK-4-induced cell growth inhibition was lower than sodium orthovanadate, a control chemotherapeutic agent, and the difference of their inhibitory activities slightly increased over time, which could be a downside of AK-4 since time-dependent anticancer effect of an anti-glioblastoma agent would be prolongated at low concentration. Nevertheless, this can be enhanced by applying combination chemotherapy, simultaneous administration of multiple anticancer drugs for obtaining long-term effect [86]. Additionally, the difference in time-dependent anticancer activities of AK-4 on both cell lines indicates that the expression of AK-4 can be altered depending on cell lines.

In the study of migration, an essential process involved in metastasis, the scratch assay was applied to evaluate the migration of glioblastoma cells treated with AK-4 in a time-dependent manner. Over 8 hours, both the cell lines in AK-4 treatment inhibited significantly scratch closure, representing for the migration of cancer cells. This is in alignment with previous studies that quinic acid derivatives are capable of inhibiting migration of cancer cells as breast, liver, lung cancer cells [17,84,87]. In addition, the antimigration capability of AK-4 was comparable to control chemotherapeutic agent after 8 hours of treatment. It is also noted that the cells started detaching from plate and the reason for detachment is relatively vague. It is assumed that the cells were dead and detached from plates. This explanation could be acceptable; however, there was no evidence supporting this assumption due to the limited scope of experiment. In case of AK-4-induced cell detachment, detaching of cancer cells *in vivo* could increase the risk of metastasis. Hence, future studies are required to clarify whether AK-4 reduces the cell adhesion and increases the cellular attachment. Besides, the concentration of FBS in complete culture

medium was decreased from 10 % as usual to 5 % to minimize the influence of cell proliferation on scratch closure as well as migration results.

It is worth considering that AK-4 increased remarkably ROS generation in both the cell lines, especially in LN229. This is totally in alignment with many studies mentioning that the elevated ROS level plays a major role in induction of glioblastoma cell death [88,89]. Additionally, it is proven by afore studies that the increase of ROS level is associated with apoptosis induction [90,91]. Hence, it is proposed that AK-4 could be promising anticancer drug inducing the cell death via apoptosis. In fact, the fragmentation was observed in LN229 treated with AK-4 after 48-h drug exposure as illustrated in Figure 11. This result is in agreement with afore study on morphologic hallmarks of cell apoptosis including cell shrinkage and fragmentation [92]. Moreover, it is proven by another study that nicotinamide, an potential anticancer drug which can be converted from quinic acid, is capable of inducing apoptosis [93]. Thus, the migration and cell death mechanism induced by AK-4 would be consistent with nicotinamide. Nonetheless, the concentration of nicotinamide (mM) as mentioned previously is much higher than concentration of AK-4 (μM). It is presumed that the presence of tert-butyldiphenylsilyl side group in AK-4 compound, which could induce apoptosis, results in the difference of effective concentration between AK-4 and nicotinamide. In order to verify this hypothesis, further examinations such as apoptosis pathway are required.

As a matter of fact, the technical errors cannot be avoided when conducting experiments in the current study; however, these errors could be minimized by repeating experiment. In specific, each treatment in the trypan blue exclusion method was repeated three times and consequently, the number of viable and non-viable cells is also counted repeatedly to minimize errors. In addition, the measurement of scratch closure width in scratch assay was also performed repeatedly at each time point.

Overall, the results found in this study have pointed out that AK-4 compound can potentially be anti-glioblastoma multiforme agent, providing alternatively effective drug for glioblastoma multiforme treatment. Nevertheless, further studies about cell death mechanism are required to clarify whether cell death was induced by apoptosis or necrosis as well as the detachment of cell in migration assay. Besides, computational modelling and nanomedicine can be applied in experiments to investigate the effect of quinic acid-conjugated nanoparticle on glioblastoma cell lines.

6. CONCLUSION

In this thesis, the promising anti-glioblastoma activity of quinic acid derivatives was characterized by a series of preclinical screenings. Quinic acid derivatives are well known to possess a wide spectrum of antitumor, antioxidant, anti-inflammatory properties; notwithstanding, the number of researches about their efficacy on glioblastoma has been very limited. In addition, the adverse effects caused by available anti-glioblastoma agents or the failures of potential agents in clinical trials have necessitated the urge to develop the novel agent for glioblastoma treatment.

In accordance with data presented in drug screening, AK-4 compound (C39H50O5Si2) displayed strong cytotoxic capability against the growth of two glioblastoma cell lines LN229 and SNB19 over other quinic acid derivatives with IC_{50} concentration of 10.6 and 28.2 μM, respectively. This implies that AK-4 induced higher cytotoxic effect rather than TMZ, the most common anti-glioblastoma agents in the same cell lines. The presence of tert-butyldiphenylsilyl group is hypothesized to enhance considerably the cytotoxicity of AK-4 compound. Moreover, as a potential anti-glioblastoma agent, the selectivity of quinic acid derivative towards non-cancerous cell lines was also taken into account and hence augmented by cytotoxicity assay on mouse embryonic fibroblast cell line. The results acquired from this assay indicated that AK-4 exhibited lower cytotoxic effect on normal cells than glioblastoma cells. It is strongly believed that with additional targeting, AK-4 is able to reach the cytotoxic threshold with minimal effect on non-cancerous cells and turn out to be more selective towards the cancer cells. Furthermore, cytotoxicity of AK-4 was also ascertained in the patient-derived glioblastoma cell lines, bearing a close resemblance to patient glioblastoma genome. According to obtained data in this assay, AK-4 was proved to induce notably inhibitory effect against the growth of MMK1 and RN1, in which cytotoxicity was found to be approximately 90 % in both the cell lines. Besides, the scratch assays in LN229 and SNB19 unveiled the significant inhibitory effect of AK-4 against scratch closure. This proved the ability of AK-4 to hinder the migration of glioblastoma cells as well as impede their metastasis. In comparison with sodium orthovanadate, control chemotherapeutic agent, AK-4 exhibited comparable antimigration capability over 8 h post-treatment. Lastly, the elevated ROS level, found in glioblastoma cells, revealed that AK-4 possessed capability of triggering glioblastoma cell death.

In conclusion, this thesis demonstrates scientific rationale to develop AK-4 based chemo-therapeutic agent as a novel class of anti-glioblastoma agents.

REFERENCES

[1] Gladson CL, Prayson RA, Liu WM. The Pathobiology of Glioma Tumors. Annu Rev Pathol Mech Dis. 2010 Jan;5(1):33–50.

[2] Zong H, Verhaak RGW, Canolk P. The cellular origin for malignant glioma and prospects for clinical advancements. Vol. 12, Expert Review of Molecular Diagnostics. NIH Public Access; 2012. p. 383–94.

[3] Louis DN, Perry A, Reifenberger · Guido, Von Deimling A, Figarella-Branger D, Webster ·, Cavenee K, Ohgaki H, Otmar ·, Wiestler D, Kleihues P, David ·, Ellison W. The 2016 World Health Organization Classification of Tumors of the Central Nervous System: a summary. Acta Neuropathol.

[4] Liu Z, Yang X, Chen C, Liu B, Ren B, Wang L, Zhao K, Yu S, Ming H. Expression of the Arp2/3 complex in human gliomas and its role in the migration and invasion of glioma cells. Oncol Rep. 2013 Nov 1;30(5):2127–36.

[5] Perazzoli G, Prados J, Ortiz R, Caba O, Cabeza L, Berdasco M, Gónzalez B, Melguizo C. Temozolomide Resistance in Glioblastoma Cell Lines: Implication of MGMT, MMR, P-Glycoprotein and CD133 Expression. 2015;

[6] Kourelis T V., Buckner JC, Gangat N, Patnaik MM. Temozolomide induced bone marrow Suppression-A single institution outcome analysis and review of the literature. Am J Hematol. 2015 Sep 1;90(9):E183–4.

[7] Francenia Santos-Sánchez N, Salas-Coronado R, Hernández-Carlos B, Villanueva-Cañongo C. Shikimic Acid Pathway in Biosynthesis of Phenolic Compounds. In: Plant Physiological Aspects of Phenolic Compounds. IntechOpen; 2019.

[8] Pero RW. Health consequences of catabolic synthesis of hippuric acid in humans. Curr Clin Pharmacol. 2010;5(1):67–73.

[9] Godin SK, Lee AG, Baird JM, Herken BW, Bernstein KA. Tryptophan biosynthesis is important for resistance to replicative stress in Saccharomyces cerevisiae. Yeast. 2016 May 1;33(5):183–9.

[10] Pero RW, Lund H, Leanderson T. Antioxidant metabolism induced by quinic acid. increased urinary excretion of tryptophan and nicotinamide. Phyther Res. 2009 Mar;23(3):335–46.

[11] Fricker RA, Green EL, Jenkins SI, Griffin SM. The Influence of Nicotinamide on Health and Disease in the Central Nervous System. Vol. 11, International Journal of Tryptophan Research. SAGE Publications Ltd; 2018.

[12] Padmini E, Inbathamizh L. Quinic acid as a potent drug candidate for prostate cancer - a comparative pharmacokinetic approach. Asian J Pharm Clin Res. 2013 Jan;6(4):106–12.

[13] Park M, Hong J. Roles of NF-κB in Cancer and Inflammatory Diseases and Their Therapeutic Approaches. Cells. 2016 Mar 29;5(2):15.

[14] Distribution of Quinic Acid Derivatives and Other Phenolic Compounds in Brazilian Propolis in: Zeitschrift für Naturforschung C Volume 58 Issue 7-8 (2003).

[15] Chung I-M, Kim M-Y, Park W-H, Moon H-I. Quinic acid derivatives from Saussurea triangulata attenuates glutamate-induced neurotoxicity in primary cultured rat cortical cells. J Enzym Inhib Med Chem. 2009;24(1):188–91.

[16] Liu ZH, Zhang SY, Yu YY, Su GQ. (-)-4-O-(4-O-β-D-glucopyranosylcaffeoyl)quinic acid presents antitumor activity in HT-29 human colon cancer in vitro and in vivo. Mol Cell Toxicol. 2015 Dec 1;11(4):457–63.

[17] Tan S, Dong X, Liu D, Hao S, He F. Anti-tumor activity of chlorogenic acid by regulating the mTORC2 signaling pathway and disrupting F-actin organization. Vol. 12, Int J Clin Exp Med. 2019.

[18] Mason JS. Computational screening: Large-scale drug discovery. Trends Biotechnol. 1999 Jan 1;17(SUPPL.1):34–6.

[19] Jeon JS, Kim HT, Jeong IH, Hong SR, Oh MS, Yoon MH, Shim JH, Jeong JH, Abd El-Aty AM. Contents of chlorogenic acids and caffeine in various coffee-related products. J Adv Res. 2019 May 1;17:85–94.

[20] Lin LZ, Harnly JM. Identification of hydroxycinnamoylquinic acids of arnica flowers and burdock roots using a standardized LC-DAD-ESI/MS profiling method. J Agric Food Chem. 2008 Nov 12;56(21):10105–14.

[21] Chan EWC, Lim YY, Tan SP. Standardised herbal extract of chlorogenic acid from leaves of Etlingera elatior (Zingiberaceae). Pharmacognosy Res. 2011 Jul;3(3):178–84.

[22] Habtemariam S. The chemical and pharmacological basis of fenugreek (Trigonella foenum-graecum L.) as potential therapy for type 2 diabetes and associated diseases. In: Medicinal Foods as Potential Therapies for Type-2 Diabetes and Associated Diseases. Elsevier; 2019. p. 579–637.

[23] Plazas M, Andújar I, Vilanova S, Hurtado M, Gramazio P, Herraiz FJ, Prohens J. Breeding for Chlorogenic Acid Content in Eggplant: Interest and Prospects. Not Bot Horti Agrobot Cluj-Napoca. 2013;41(1):26–35.

[24] Zeng K. UTHSC Digital Commons Discovery of Quinic Acid Derivatives as Oral Anti-inflammatory Agents. 2010.

[25] Ghafourian E, Kahrarian M, Jafari F, Ghiasvand N, Jalilian F, Hosseinzadeh L, Shokoohinia Y. 2017: 68 First Iranian Pharmacognosy Congress. Vol. 4, Research Journal of Pharmacognosy (RJP).

[26] Kim KH, Kim YH, Lee KR. Isolation of quinic acid derivatives and flavonoids from the aerial parts of Lactuca indica L. and their hepatoprotective activity in vitro. Bioorganic Med Chem Lett. 2007 Dec 15;17(24):6739–43.

[27] Zeng K, Thompson KE, Yates CR, Miller DD. Synthesis and biological evaluation of quinic acid derivatives as anti-inflammatory agents. Bioorganic Med Chem Lett. 2009 Sep 15;19(18):5458–60.

[28] Russo A, Fratto ME, Bazan V, Schirò V, Agnese V, Cicero G, Vincenzi B, Tonini G, Santini D. Targeting apoptosis in solid tumors: The role of bortezomib from preclinical to clinical evidence. Vol. 11, Expert Opinion on Therapeutic Targets. 2007. p. 1571–86.

[29] Pucci B, Kasten M, Giordano A. Cell cycle and apoptosis. Vol. 2, Neoplasia. Neoplasia Press; 2000. p. 291–9.

[30] Overholtzer M, Mailleux AA, Mouneimne G, Normand G, Schnitt SJ, King RW, Cibas ES, Brugge JS. A nonapoptotic cell death process, entosis, that occurs by cell-in-cell invasion. Cell. 2007 Nov 30;131(5):966–79.

[31] Elmore S. Apoptosis: A Review of Programmed Cell Death. Vol. 35, Toxicologic Pathology. NIH Public Access; 2007. p. 495–516.

[32] Norbury CJ, Hickson ID. Cellular response to DNA Damage. Annu Rev Pharmacol Toxicol. 2001 Apr;41(1):367–401.

[33] Hirsch T, Marchetti P, Susin SA, Dallaporta B, Zamzami N, Marzo I, Geuskens M, Kroemer G. The apoptosis-necrosis paradox. Apoptogenic proteases activated after mitochondrial permeability transition determine the mode of cell death. Oncogene. 1997;15(13):1573–81.

[34] Zeiss CJ. The apoptosis-necrosis continuum: Insights from genetically altered mice. Vol. 40, Veterinary Pathology. Vet Pathol; 2003. p. 481–95.

[35] Häcker G. The morphology of apoptosis. Vol. 301, Cell and Tissue Research. Springer Verlag; 2000. p. 5–17.

[36] Kerr JFR, Wyllie AH, Currie AR. Apoptosis: A basic biological phenomenon with wide-ranging implications in tissue kinetics. Br J Cancer. 1972;26(4):239–57.

[37] Savill J, Fadok V. Corpse clearance defines the meaning of cell death. Vol. 407, Nature. Nature; 2000. p. 784–8.

[38] Kurosaka K, Takahashi M, Watanabe N, Kobayashi Y. Silent Cleanup of Very Early Apoptotic Cells by Macrophages. J Immunol. 2003 Nov 1;171(9):4672–9.

[39] Apoptosis mediated by mitochondria - Cusabio [Internet]. [cited 2020 Apr 13]. Available from: https://www.cusabio.com/c-20458.html

[40] Igney FH, Krammer PH. Death and anti-death: Tumour resistance to apoptosis. Vol. 2, Nature Reviews Cancer. Nat Rev Cancer; 2002. p. 277–88.

[41] Loreto C, La Rocca G, Anzalone R, Caltabiano R, Vespasiani G, Castorina S, Ralph D , Cellek S, Musumeci G, Giunta S, Djinovic R, Basic D, Sansalone S. The Role of Intrinsic Pathway in Apoptosis Activation and Progression in Peyronie's Disease. Biomed Res Int. 2014;2014.

[42] Saelens X, Festjens N, Vande Walle L, Van Gurp M, Van Loo G, Vandenabeele P. Toxic proteins released from mitochondria in cell death. Vol. 23, Oncogene. Oncogene; 2004. p. 2861–74.

[43] Du C, Fang M, Li Y, Li L, Wang X. Smac, a mitochondrial protein that promotes cytochrome c-dependent caspase activation by eliminating IAP inhibition. Cell. 2000 Jul 7;102(1):33–42.

[44] Chinnaiyan AM. The apoptosome: heart and soul of the cell death machine. Vol. 1, Neoplasia (New York, N.Y.). Neoplasia; 1999. p. 5–15.

[45] Hill MM, Adrain C, Duriez PJ, Creagh EM, Martin SJ. Analysis of the composition, assembly kinetics and activity of native Apaf-1 apoptosomes. EMBO J. 2004 May 19;23(10):2134–45.

[46] Morita A, Yamamoto S, Wang B, Tanaka K, Suzuki N, Aoki S, Ito A, Nanao T, Ohya S, Yoshino M, Zhu J, Enomoto A, Matsumoto Y, Funatsu O, Hosoi Y, Ikekita M. Sodium orthovanadate inhibits p53-mediated apoptosis. Cancer Res. 2010 Jan 1;70(1):257–65.

[47] Joza N, Susin SA, Daugas E, Stanford WL, Cho SK, Li CYJ, Sasaki T, Elia AJ, Cheng HYM, Ravagnan L, Ferri KF, Zamzami N, Wakeham A, Hakem R, Yoshida H, Kong YY, Mak TW, Zúñiga-Pflücker JC, Kroemer G, et al. Essential role of the mitochondrial apoptosis-inducing factor in programmed cell death. Nature. 2001 Mar 29;410(6828):549–54.

[48] Li LY, Luo X, Wang X. Endonuclease G is an apoptotic DNase when released from mitochondria. Nature. 2001 Jul 5;412(6842):95–9.

[49] Locksley RM, Killeen N, Lenardo MJ. The TNF and TNF receptor superfamilies: Integrating mammalian biology. Vol. 104, Cell. Cell Press; 2001. p. 487–501.

[50] Chicheportiche Y, Bourdon PR, Xu H, Hsu YM, Scott H, Hession C, Garcia I, Browning JL. TWEAK, a new secreted ligand in the tumor necrosis factor family that weakly induces apoptosis. J Biol Chem. 1997 Dec 19;272(51):32401–10.

[51] Denecker G, Vercammen D, Declercq W, Vandenabeele P. Apoptotic and necrotic cell death induced by death domain receptors. Vol. 58, Cellular and Molecular Life Sciences. Birkhauser Verlag Basel; 2001. p. 356–70.

[52] Weerasinghe P, Buja LM. Oncosis: an important non-apoptotic mode of cell death. Exp Mol Pathol. 2012 Dec;93(3):302–8.

[53] Trump BF, Berezesky IK, Chang SH, Phelps PC. The pathways of cell death:

Oncosis, apoptosis, and necrosis. In: Toxicologic Pathology. SAGE Publications Inc.; 1997. p. 82–8.

[54] Cell Death | BioNinja [Internet]. [cited 2020 Apr 14]. Available from: http://www.vce.bioninja.com.au/aos-3-heredity/cell-reproduction/cell-death.html

[55] Proskuryakov SY, Konoplyannikov AG, Gabai VL. Necrosis: A specific form of programmed cell death? Vol. 283, Experimental Cell Research. Academic Press Inc.; 2003. p. 1–16.

[56] Hastie T, Tibshirani R, Friedman J. Springer Series in Statistics The Elements of Statistical Learning Data Mining, Inference, and Prediction.

[57] Doan P, Musa A, Murugesan A, Sipilä V, Candeias NR, Emmert-Streib F, Ruusuvuori P, Granberg K, Yli-Harja O, Kandhavelu M. Glioblastoma Multiforme Stem Cell Cycle Arrest by Alkylaminophenol Through the Modulation of EGFR and CSC Signaling Pathways. Cells. 2020 Mar 10;9(3):681.

[58] Attardi LD, De Vries A, Jacks T. Activation of the p53-dependent G1 checkpoint response in mouse embryo fibroblasts depends on the specific DNA damage inducer. Oncogene. 2004;23(4):973–80.

[59] Xu W, Baribault H, Adamson ED. Vinculin knockout results in heart and brain defects during embryonic development. Development. 1998;125(2):327–37.

[60] Delwar ZM, Avramidis D, Follin E, Hua Y, Siden Å, Cruz M, Paulsson KM, Yakisich JS. Cytotoxic effect of menadione and sodium orthovanadate in combination on human glioma cells. Invest New Drugs. 2012 Aug 10;30(4):1302–10.

[61] Wu Y, Ma Y, Xu Z, Wang D, Zhao B, Pan H, Wang J, Xu D, Zhao X, Pan S, Liu L, Dai W, Jiang H. Sodium orthovanadate inhibits growth of human hepatocellular carcinoma cells in vitro and in an orthotopic model in vivo. Cancer Lett. 2014 Aug 28;351(1):108–16.

[62] Jain MR, Bandyopadhyay D, Sundar R. Scientific and Regulatory Considerations in the Development of in Vitro Techniques for Toxicology. In: In Vitro Toxicology. Elsevier Inc.; 2018. p. 165–85.

[63] Tran SL, Puhar A, Ngo-Camus M, Ramarao N. Trypan blue dye enters viable cells incubated with the pore-forming toxin HlyII of Bacillus cereus. PLoS One.

2011;6(9).

[64] Campbell JE, Cohall D. Pharmacodynamics-A Pharmacognosy Perspective. In: Pharmacognosy: Fundamentals, Applications and Strategy. Elsevier Inc.; 2017. p. 513–25.

[65] Hulkower KI, Herber RL. Cell migration and invasion assays as tools for drug discovery. Vol. 3, Pharmaceutics. Multidisciplinary Digital Publishing Institute (MDPI); 2011. p. 107–24.

[66] Liang CC, Park AY, Guan JL. In vitro scratch assay: A convenient and inexpensive method for analysis of cell migration in vitro. Nat Protoc. 2007 Mar 1;2(2):329–33.

[67] Moutasim KA, Nystrom ML, Thomas GJ. Cell Migration and Invasion Assays. In 2011. p. 333–43.

[68] Pearson JRD, Regad T. Targeting cellular pathways in glioblastoma multiforme. Vol. 2, Signal Transduction and Targeted Therapy. Springer Nature; 2017. p. 17040.

[69] Assays kits Reactive Oxygen Species Assay Kit.

[70] Roesslein M, Hirsch C, Kaiser JP, Krug HF, Wick P. Comparability of in vitro tests for bioactive nanoparticles: A common assay to detect reactive oxygen species as an example. Int J Mol Sci. 2013 Dec 13;14(12):24320–37.

[71] Day BW, Stringer BW, Al-Ejeh F, Ting MJ, Wilson J, Ensbey KS, Jamieson PR, Bruce ZC, Lim YC, Offenhäuser C, Charmsaz S, Cooper LT, Ellacott JK, Harding A, Leveque L, Inglis P, Allan S, Walker DG, Lackmann M, et al. EphA3 Maintains Tumorigenicity and Is a Therapeutic Target in Glioblastoma Multiforme. Cancer Cell. 2013 Feb 11;23(2):238–48.

[72] Pollard SM, Yoshikawa K, Clarke ID, Danovi D, Stricker S, Russell R, Bayani J, Head R, Lee M, Bernstein M, Squire JA, Smith A, Dirks P. Glioma Stem Cell Lines Expanded in Adherent Culture Have Tumor-Specific Phenotypes and Are Suitable for Chemical and Genetic Screens. Cell Stem Cell. 2009 Jun 5;4(6):568–80.

[73] Chang MC, Wu JY, Liao HF, Chen YJ, Kuo CD. Comparative assessment of therapeutic safety of norcantharidin, N -farnesyloxy-norcantharimide, and N -farnesyl-norcantharimide against Jurkat T cells relative to human normal

lymphoblast: A quantitative pilot study. Med (United States). 2016 Aug 1;95(31).

[74] Yang X, Xu Y, Wang T, Shu D, Guo P, Miskimins K, Qian SY. Inhibition of cancer migration and invasion by knocking down delta-5-desaturase in COX-2 overexpressed cancer cells. Redox Biol. 2017 Apr 1;11:653–62.

[75] Guan X. Cancer metastases: Challenges and opportunities. Vol. 5, Acta Pharmaceutica Sinica B. Chinese Academy of Medical Sciences; 2015. p. 402–18.

[76] Liou GY, Storz P. Reactive oxygen species in cancer. Vol. 44, Free Radical Research. Informa Healthcare; 2010. p. 479–96.

[77] Kumari S, Badana AK, Murali Mohan G, Shailender G, Malla RR. Reactive Oxygen Species: A Key Constituent in Cancer Survival. Vol. 13, Biomarker Insights. SAGE Publications Ltd; 2018.

[78] Redza-Dutordoir M, Averill-Bates DA. Activation of apoptosis signalling pathways by reactive oxygen species. Vol. 1863, Biochimica et Biophysica Acta - Molecular Cell Research. Elsevier B.V.; 2016. p. 2977–92.

[79] Stringer BW, Day BW, D'Souza RCJ, Jamieson PR, Ensbey KS, Bruce ZC, Lim YC, Goasdoué K, Offenhäuser C, Akgül S, Allan S, Robertson T, Lucas P, Tollesson G, Campbell S, Winter C, Do H, Dobrovic A, Inglis PL, et al. A reference collection of patient-derived cell line and xenograft models of proneural, classical and mesenchymal glioblastoma. Sci Rep. 2019 Dec 1;9(1):1–14.

[80] Zeng K, Thompson KE, Yates CR, Miller DD. Synthesis and biological evaluation of quinic acid derivatives as anti-inflammatory agents. Bioorganic Med Chem Lett. 2009 Sep 15;19(18):5458–60.

[81] Patent U. Sheet 1 of 12 US 8,115,031 B2. 2012.

[82] Apryshko GN, Filimonov DA, Poroykov V V, Rickardson LR, Larsson R, Lövborg H, Padrón JM, Donadel OJ, Martín T, Martín VS, Villar J. Poster session 1: Drug design and screening p.101 The computer-aided prediction of small molecule substances interaction with the biological targets of anticancer agents p.102 high -content screening for the indentification of novel proteasome inhibitors. 2005.

[83] WHO Drug Information Vol. 19, No. 2, 2005: Regulatory Action and News:

Temozolomide approved for glioblastoma multiforme.

[84] Yagasaki K, Miura Y, Okauchi R, Furuse T. Inhibitory effects of chlorogenic acid and its related compounds on the invasion of hepatoma cells in culture. Cytotechnology. 2000;33(1–3):229–35.

[85] Stringer BW, Day BW, D'Souza RCJ, Jamieson PR, Ensbey KS, Bruce ZC, Lim YC, Goasdoué K, Offenhäuser C, Akgül S, Allan S, Robertson T, Lucas P, Tollesson G, Campbell S, Winter C, Do H, Dobrovic A, Inglis PL, et al. A reference collection of patient-derived cell line and xenograft models of proneural, classical and mesenchymal glioblastoma. Sci Rep. 2019 Dec 1;9(1).

[86] Hu Q, Sun W, Wang C, Gu Z. Recent advances of cocktail chemotherapy by combination drug delivery systems. Vol. 98, Advanced Drug Delivery Reviews. Elsevier B.V.; 2016. p. 19–34.

[87] Metaferia BB, Chen L, Baker HL, Huang XY, Bewley CA. Synthetic macrolides that inhibit breast cancer cell migration in vitro. J Am Chem Soc. 2007 Mar 7;129(9):2434–5.

[88] A Snezhkina A, Kudryavtseva A, Kardymon O, Savvateeva M, Melnikova N, Krasnov G, Dmitriev A. ROS Generation and Antioxidant Defense Systems in Normal and Malignant Cells. Oxid Med Cell Longev. 2019 Aug 5;2019:6175804–6175804.

[89] Rinaldi M, Caffo M, Minutoli L, Marini H, Abbritti RV, Squadrito F, Trichilo V, Valenti A, Barresi V, Altavilla D, Passalacqua M, Caruso G. ROS and brain gliomas: An overview of potential and innovative therapeutic strategies. Vol. 17, International Journal of Molecular Sciences. MDPI AG; 2016.

[90] Simon HU, Haj-Yehia A, Levi-Schaffer F. Role of reactive oxygen species (ROS) in apoptosis induction. Apoptosis. 2000;5(5):415–8.

[91] Circu ML, Aw TY. Reactive oxygen species, cellular redox systems, and apoptosis. Vol. 48, Free Radical Biology and Medicine. 2010. p. 749–62.

[92] Saraste A, Pulkki K. Morphologic and biochemical hallmarks of apoptosis. Vol. 45, Cardiovascular Research. Oxford Academic; 2000. p. 528–37.

[93] Wang Y, Ryu HS, Jang JJ. Nicotinamide suppresses cell growth by G1-phase

arrest and induces apoptosis in intrahepatic cholangiocarcinoma. Mol Cell Toxicol. 2018 May;14(1):43–51.

APPENDIXES A

A.1 Supplemented figures

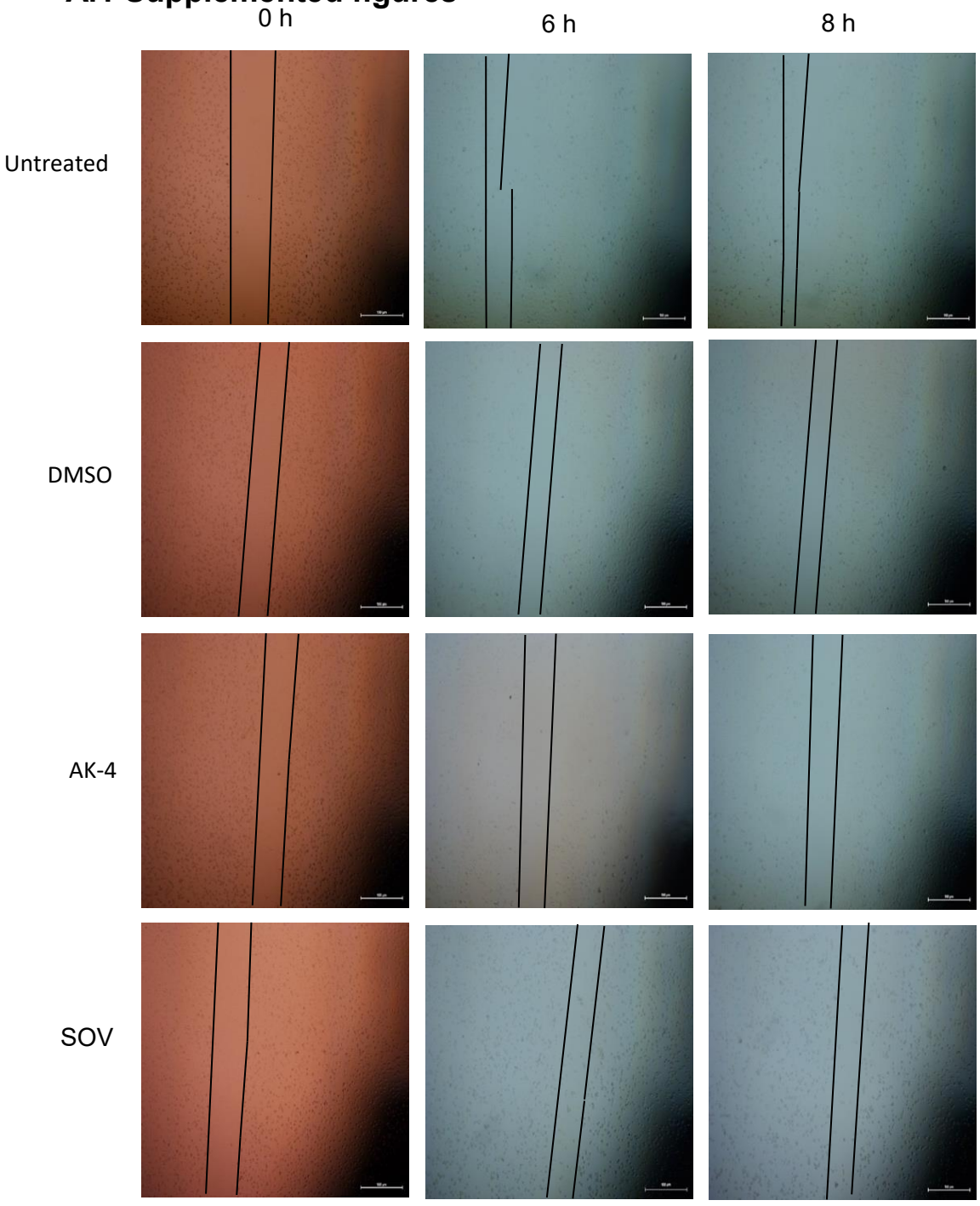

Figure A.1. Examples of photomicrographs showing closing of scratched area in untreated LN229 cells and DMSO, AK-4, sodium orthovanadate – treated cells at 0, 6, 8 h post-treatment.

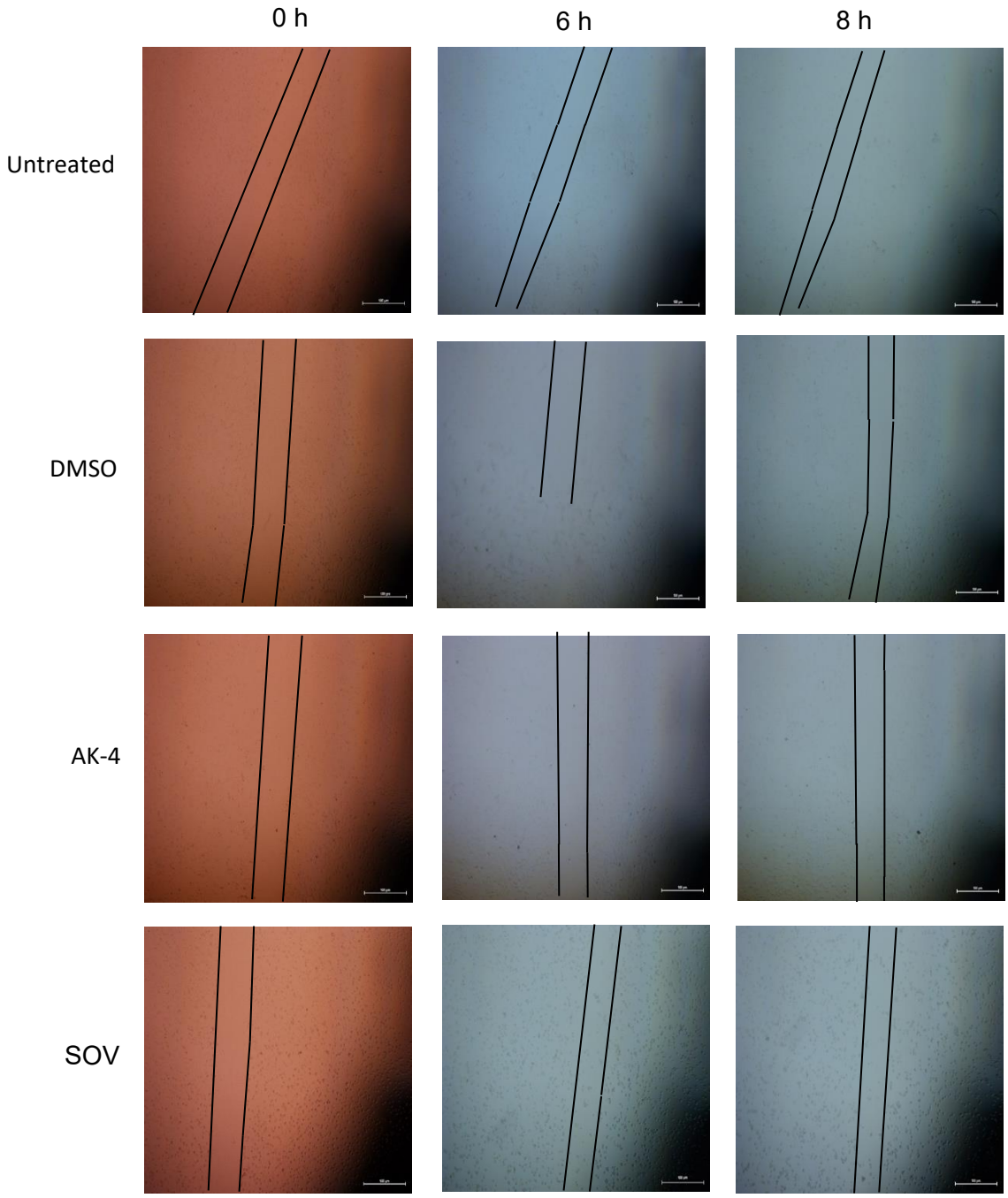

Figure A.2. Examples of photomicrographs showing closing of scratched area in untreated SNB19 cells and DMSO, AK-4, sodium orthovanadate (SOV) – treated cells at 0, 6, 8 h post-treatment.

A.2 Experimental results

Table A.1. Cell growth inhibition of 16 quinic acid derivatives and negative control at 100 μM on LN229

Compounds	**Cell growth inhibition (%)**
NC	-1.68 ± 10,99
SHA-82	20.22±16.63
AK-7	5.54±3.62
SHA-161	53.14±10.42
SHA-181	48.90±17.14
SHA-111	-6.71±9.50
AK-17	-4.68±11.90
SHA-159	49.99±11.08
SHA-171	37.79±23.10
SHA-150	-0.01±11.89
AK-4	90.12±5.10
AK-8	30.78±7.60
AK-22	-6.41±10.89
SHA-222	-11.29±10.01
SHA-272	-6.43±8.30
AK-15A	-9.66±10.97
AK-15B	-9.51±10.04

Table A.2. Dose dependent effect of AK-4 on cell lines LN229 and SNB19

Concetration (μM)	Cell growth inhibition (%)	
	Cell line LN229	Cell line SNB19
0	11,01±4.55	9.31±1.46
25	78.24±6.81	18.15±2.62
50	86.73±3.38	95.39±1.78
75	93.65±2.57	92.36±1.48
100	92.92±5.51	94.69±2.28

Table A.3. Time dependent effect of AK-4 on cell lines LN229 and SNB19

Time	Cell growth inhibition (%)			
	LN229		SNB19	
	AK-4	Sodium ortho-vanadate	AK-4	Sodium ortho-vanadate
24	20.18±11.19	70.59±7.25	43.35±7.83	57.95±7.87
48	32.08±7.19	90.12±6.68	45.74±9.26	62.22±7.26
72	38.48±14.6	98.85±0.86	53.86±7.06	81.27±6.21

Table A.4. Effect of AK-4 on scratch closure ass in LN229

Time	Scratch closure in LN229 (%)			
	Untreated	DMSO	AK-4	SOV
2	9.3±6.1	32.5±3.5	28.8±1.3	15.3±6.7
4	18.6±12.2	25.0±0	30.1±4.4	20.5±0.7
6	33.0±11.2	35.5±7.1	26.5±4.4	30.8±1.1
8	49.8±6.7	47.5±3.5	27.6±9.4	30.7±6.1
24	100±0	100±0		33.6±12.1

Table A.5. Scratch closure in SNB19

Time	Scratch closure in SNB19 (%)			
	Untreated	DMSO	AK-4	SOV
2	11.8±3.6	7.1±7.1	3.6±5.1	5.9±5.9
4	14.3±10.2	13.7±14.3	11.3±4.1	12±5.5
6	21.4±8.5	23.3±3.8	15.1±6.3	12±5.5
8	25.2±8.4	28.6±1.7	15.0±5.6	14.2±3
24	35.8±10.9	31.8±7.5		14.2±3

Table A.6. ROS generation on LN229 and SNB19

Compound		
	LN229	**SNB19**
H202	2.925±0.996	1.405±0.176
AK-4	2.949±0.907	1.149±0.836